Science of the Total Environment 676 (2019) 595–612

Contents lists available at ScienceDirect

Science of the Total Environment

journal homepage: www.elsevier.com/locate/scitotenv

Assessing the water and carbon footprint of hydropower stations at a national scale

Jinyan Wang [a], Xiuzhi Chen [a], Zhongwei Liu [c], Veronica F. Frans [b], Zhenci Xu [b,*], Xinjiao Qiu [d], Feipeng Xu [a], Yunkai Li [a,*]

[a] College of Water Resources and Civil Engineering, China Agricultural University, Beijing 100083, China
[b] Center for Systems Integration and Sustainability, Department of Fisheries and Wildlife, Michigan State University, East Lansing, MI 48823, USA
[c] Division of Materials, China Institute of Water Resources and Hydropower Research (IWHR), Beijing, China
[d] Water Resources Department, Construction Management and Quality Safety Center, Beijing, Haidian 100038, China

HIGHLIGHTS

- Water and CO_2 footprint of hydropower have not been studied simultaneously at a large scale.
- We firstly assess water and CO_2 footprint of China's hydropower at a national scale.
- We include all life cycle stages of hydropower for the assessment.
- Water footprint of China's hydropower is equal to 18.9% of Yellow River's annual runoff
- Most carbon footprint is from the operation and maintenance stages

GRAPHICAL ABSTRACT

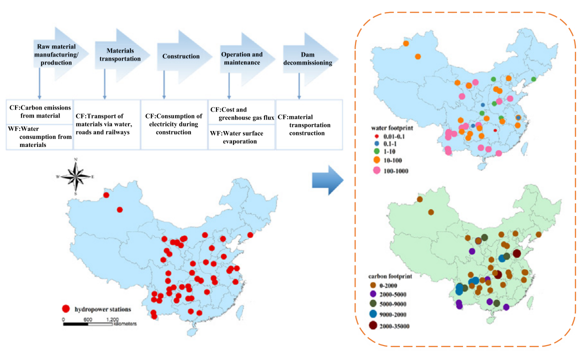

ARTICLE INFO

Article history:
Received 17 September 2018
Received in revised form 18 March 2019
Accepted 10 April 2019
Available online 22 April 2019

Editor: Deyi Hou

Keywords:
Water-energy-CO_2 nexus
Footprint
Environmental impact assessment
Life Cycle Assessment
China
Reservoir

ABSTRACT

Hydropower is among the most widely-adopted renewable energy sources worldwide. Its development has, however, led to environmental impacts such as carbon emissions and water loss. To date, the water footprint (WF) and carbon footprint (CF) of hydropower stations have been assessed, but not simultaneously or at a large scale such as national scale. Previous WF and CF studies rarely assessed all life-cycle stages of a hydropower station, calling for a more holistic understanding of the environmental impacts of hydropower. We developed a complete WF and CF assessment method and applied it to a case study on 50 of China's most influential hydropower stations, representing over 80% of the country's total hydropower. The total annual WF of these hydropower stations was 5.50×10^{11} m^3, equal to 18.9% of Yellow River's annual runoff. The total CF of these stations was 1.06×10^7 tCO_2e, with extremely large variations found, ranging from 1850 to 1.56×10^6 tCO_2e. This study provides the first environmental impact assessment to simultaneously include the WF and CF of multiple influential hydropower stations at a national scale. We were able to show spatial variations in their environmental impacts from different life-cycle stages of the hydropower station. Most of the WF was due to surface water loss from reservoirs, while most of the CF was derived from the operational and maintenance stage of these stations. This initial WF and CF assessment of hydropower at a national scale provides insights for water resource management and carbon reduction during hydropower development.

* Corresponding authors.
E-mail addresses: xuzhencinl@gmail.com (Z. Xu), liyunkai@126.com (Y. Li).

https://doi.org/10.1016/j.scitotenv.2019.04.148

1. Introduction

The world's environmental and socioeconomic sustainability is facing unprecedented challenges as a result of the global energy and water crisis (Rothausen and Conway, 2011). Worldwide, more than one billion people lack access to electricity (International Energy Agency, 2015), and four billion people face water scarcity (Mekonnen and Hoekstra, 2016). Economic development and population growth, coupled with energy-water nexus, present further challenges to resilient infrastructure development. Hydropower has been proposed as a potential solution, due to its advantages on improving resource utilization and bringing socio-economic benefits (Barnaby, 2009). It currently accounts for 71% of global renewable energy (Edenhofer et al., 2013), contributing to almost 100%, over 80%, and over 50% of national electricity in 13, 32, and 65 countries, respectively (Yüksel, 2009).

Hydropower is considered by some to be the most important type of renewable energy (Wüstenhagen et al., 2007; Mekonnen et al., 2016). It satisfies renewable energy demands under climate change policies and can bring substantial economic benefits (Delucchi and Jacobson, 2011). Hydropower has been developed and used in many countries worldwide (Fthenakis and Kim, 2010). According to the 2013 World Renewable Energy Development Report (2014), hydropower makes up to 85% of the world's renewable energy. There are 65 countries around the world that rely on hydropower to support >50% of their national electricity, of which 32 countries rely on hydropower for >80% of their national electricity, and 13 countries rely on hydropower for almost 100% of their national electricity (Yüksel, 2009).

Recently, however, some studies have found that hydroelectric reservoirs are a large source of greenhouse gas (GHG) emissions (Shakya and Shrestha, 2011; Li et al., 2009; Zhang et al., 2015). There is also growing concern about water loss in hydropower development (Gleick, 1992). Comprehensive methods assessing the environmental impacts of hydropower stations from a life-cycle perspective are thus urgently needed. Water footprint (WF) and carbon footprint (CF) are among the promising tools to assess water consumption (Gerbensleenes et al., 2009) and carbon emissions across the life cycle of hydropower stations. Various studies have assessed the WF and CF of hydropower stations. Nevertheless, most of these studies did not provide a full life-cycle assessment and tend to focus only on the operational stage (Gleick, 1993; Hung and Ma, 2009), leading to a possible underestimation of WF and CF. As a result of these limitations, governments lack a complete picture of the environmental impacts of hydropower stations, risking an incomplete understanding of hydropower development for policy management. Furthermore, fewer studies embraced a geographic coverage of China, which has the largest hydropower development project in since 1994 (the three George reservoir) and has one of the worlds' oldest hydropower stations (Dujiangyan). More importantly, no research has simultaneously studied the WF and CF of hydropower stations at a national scale for China.

Many footprint indicators have been proposed to assess human impacts on the earth's environment (Chapagain and Hoekstra, 2002; Galli et al., 2012; Mekonnen and Hoekstra, 2011; Wackernagel, 1999). For example, the water footprint (WF) concept provides a method to estimate the water resources consumed by products and services over a given period of time (Chapagain and Hoekstra, 2002; Mekonnen and Hoekstra, 2011; Pellicer-Martínez and Martínez-Paz, 2016). Another well-known tool, the carbon footprint (CF) concept, relates GHG emissions relevant to climate change with human production or consumption activities (Wiedmann and Minx, 2009). With regard to hydropower, both of these concepts can be used as important indicators to assess water consumption (Gerbensleenes et al., 2009) and carbon emissions across the life cycle of these stations.

Some studies have assessed the water and carbon footprints of hydropower stations (Bueno et al., 2016; Zhao and Liu, 2015; Prairie et al., 2017; Zhang et al., 2015). For example, Gleick (1992) used the evaporation of reservoirs to measure the WF of hydropower stations around the world. Herath et al. (2011) used net water consumption theory and net water balance theory to estimate the average WF of power generated in a hydropower station in New Zealand. However, they did not assess all stages of the hydropower life cycle. For example, Gleick (1993) focused on water consumed due to water evaporation during hydropower station operation, but they did not considered the water consumption from construction and material manufacturing. Similarly, the construction stage was excluded from a hydropower station reservoir CF study by Hung et al. (2009), leading to a possible underestimation of carbon emissions. As a result of these limitations, governments lack a complete picture of the environmental impacts of hydropower stations, risking an incomplete understanding of hydropower development for policy management.

A comprehensive assessment that includes all stages of the hydropower station life cycle is urgently needed. More importantly, no research has simultaneously studied the water and carbon footprints of hydropower stations at a national scale for China. As more hydropower stations are being developed in response to energy shortages and climate change (Soito, 2011), such information is critically needed. A large-scale, spatially-explicit analysis of the environmental impact of hydropower stations can therefore provide useful information for governments to manage the construction and operation hydropower stations and maximize their function and benefits while lowering its environmental impacts. A more complete assessment, covering a broader scope of stages during the hydropower stations life cycle can also present a more comprehensive picture of the environmental impacts of developing hydropower (Min and Zhang, 2003).

To fill these knowledge gaps, we selected 50 of China's most influential hydropower stations as a first demonstration. These 50 stations are the largest hydropower stations located across China (Fig. 1). We aimed to solve the following questions: (1) *what is the total WF and* CF *of all these hydropower stations?* (2) *What is the WF and* CF *of each stage during the life cycle of these hydropower stations?* (3) *What is the relationship between the WF and* CF *of these hydropower stations?* We also developed a complete assessment that accounts for the WF and CF from all life-cycle stages of the hydropower stations. Further, we provide policy recommendations for the development and utilization of hydropower stations in the future.

2. Materials and methods

2.1. Study area and data sources

For this study, we selected 50 of China's largest and most influential hydropower stations (Fig. 1; see Appendix A for hydropower station names). They generate 81.21% of the nation's annual hydropower (Zheng, 2006), and account for over 78% of the total national installed capacity. The geographic distribution of these hydropower stations is shown in Fig. 1.

We used monthly meteorological data from 48 meteorological stations in China, dating from 1981 to 2016 (China Meteorological Data Service Center; http://data.cma.cn/). We obtained data for the energy consumables involved in each stage of the hydropower stations' life cycles from data record books (e.g., *China Hydropower Project in the 21st Century*—Peng, 2006; *Water Conservancy Yearbooks 1981 to 2016*). We obtained satellite imagery from Landsat-8 (https://landsat.usgs.gov/landsat-8) for land cover classifications.

2.2. Methods for calculating the water and carbon footprint of hydropower stations

2.2.1. Water footprint (WF) calculation

The water footprint calculation for reservoir construction is based on ISO 14046-1:2006 (ISO, 2006). The calculation of the WF of each hydropower station (Ma et al., 2018) consisted of two main parts: the amount of water evaporation from the hydropower station's reservoir (WF_e),

Fig. 1. Geographic distribution of 50 of China's most influential hydropower stations. The numbers assigned to each hydropower station correspond to Appendix A, where the name, size and storage capacity of each hydropower station are listed.

and the amount of water consumed during the construction stage of the hydropower station's life cycle (WF_m). The total hydropower station WF (WF_{total}) was the sum of these two parts:

$$WF_{total} = WF_e + WF_m \tag{1}$$

To calculate WF_e (m^3), we multiplied the product of the hydropower station's reservoir water surface evaporation (E(mm)) and the hydropower station's reservoir water surface area (A(hm^2)) by 10:

$$WF_e = 10 \cdot E \cdot A \tag{2}$$

E was calculated by using a reservoir surface evaporation optimization model proposed by Min and Zhang (2003). This model extends the Penman-Monteith (PAO) model equation (Penman, 1948) into a multi-factor surface evaporation model that combines meteorological factors to estimate water surface evaporation. E was thus calculated as follows (Min and Zhang, 2003):

$$E = \Delta e \times f(\Delta T,\ r,\ W) \tag{3}$$

$$f(\Delta T,\ r,\ W) = g(\Delta T) \cdot \varphi(r) \cdot \varphi(W) \tag{4}$$

$$\varphi(W) = \begin{cases} 0.192 + 0.08W, & (W \le 1.5\ \text{m/s}) \\ 0.312 + 0.078(W-1.5)^{1-0.098(W-1.5)^{0.5}}, & (W > 1.5\ m/s) \end{cases} \tag{5}$$

$$\varphi(r) = 0.153 + 0.651\left(1-r^2\right)^{1/2} \tag{6}$$

$$g(\Delta T) = 0.92 + 0.0363\Delta T^{1.08} \tag{7}$$

$$VPD = 0.611^{\{(T_{a\times 17.27})/(T_{a+237.2})\times(1-r/100)\}} \tag{8}$$

The nomenclature for these calculations is provided in Appendix B.

The major materials used during the construction of hydropower stations included concrete, wood, steel, fuel, natural gas and explosives. In the production and processing of these raw materials, we calculated WF_m as:

$$WF_m = \sum_{i=1}^{n} \propto_i \cdot X_i, \tag{9}$$

where $\propto_i$ is the WF of material i, as defined by Bribián et al. (2011), and X_i is the amount of material i that was used.

2.2.2. Carbon footprint (CF) calculation

To calculate the CF of each hydropower station, we adopted a basic carbon emission calculation approach proposed by the United Nations Intergovernmental Panel on Climate Change (IPCC; Gleick, 1993). CF is expressed in terms of greenhouse gas emissions for specific activities calculated using CO_2 equivalents. In this approach, CF represents carbon footprint, calculated in metric tonnage of the carbon dioxide equivalent (tCO_2e).

The carbon footprint calculation formula is:

$$CF = \sum_{i=1}^{5} \beta_i \cdot R_i \tag{10}$$

where CF is the total carbon footprint in the life cycle; β_i is the carbon emission factor of a specific activity; R_i is the measure of an activity.

In this study, we adopted the Life Cycle Assessment (LCA) theory to calculate the CF of hydropower stations during all five stages of its life cycle (Ribeiro and Silva, 2010; Zhang et al., 2007): (1) raw material and equipment manufacturing or production; (2) transportation; (3) construction; (4) operation and maintenance; and (5) dam decommissioning. We calculated each hydropower station's total CF (CF_{total}) by taking the sum of the CF values across the life-cycle stages as follows:

$$CF_{total} = CF_m + CF_t + CF_c + CF_o + CF_d, \tag{11}$$

where CF_{total} is the CF from all life-cycle stages, and CF_m, CF_t, CF_c, CF_o, and CF_d are the carbon emissions from the 5 respective stages (see Appendix B for nomenclature; Moomaw et al., 2011a, 2011b).

We calculated the CF of the first stage (raw material and equipment production; CF_m) as:

$$CF_m = \sum_{i=1}^{n} M_i \cdot \gamma_i, \tag{12}$$

where γ_i is the carbon emission factor of material or equipment i summed across n types of materials or equipment, and M_i is the amount of material or equipment i. Table 1 shows a list of carbon emission factors for each material or equipment and their units of measure.

For a hydropower project, raw materials, metal structure installations and electromechanical equipment are mainly transported to the construction site by way of water, roads and railways (Peng, 2006). The CF from the transportation stage (CF_t) mainly derives from the carbon emissions emitted by fuels consumed during transport (Lu, 2015). It is the sum of the product of the distance traveled (D), the volume of the workload or material transported (W), and the carbon emission factor (EF) for each mode of transport (j; see Table 1). We thus calculated CF_t as follows (Xue and Jiang, 2004):

$$CF_t = \sum_j EF_j \cdot D \cdot W \tag{13}$$

During the third stage, construction activities (e.g., excavation, concrete pouring, curtain grouting, backfill grouting and consolidation grouting) consume fuels such as diesel or electricity and simultaneously emit carbon. To calculate the CF from the construction stage (CF_c), we first omitted fuel consumption as a factor to avoid a potential overlap (or, double-counting) in the CF_{total} estimate, as it was already included in the materials production stage (CF_m). Thus only including the electric power consumption of construction machinery (δ; Hertwich et al., 2015), we followed the formula from Zhang and Pang (2015) and calculated CF_c as:

$$CF_c = \sum\nolimits_k \delta_k \cdot M_k \cdot \tau_i, \tag{14}$$

where δ_k is the unit of electric power consumption of construction project k; M_k is the quantity of work in project k (see Peng, 2006 for details); and τ_i is the carbon emission constrants of the electricity generated in each hydropower station's respective region (Zhixu, 2013; Table 2; Appendix B).

We calculated the CF of the hydropower stations' operation and maintenance stage (CF_o) as the sum of two parts: the daily maintenance of the hydropower station (CF_{ma}) and the net GHG flux from its reservoir (CF_{net}):

$$CF_o = CF_{ma} + CF_{net} \tag{15}$$

Due to a lack of detailed data on the daily maintenance of the hydropower stations in our study area, we used the Economic Input-Output Life Cycle Assessment (EIO-LCA) method to estimate CF_{ma} (Lave, 2006). To support their operation, hydropower stations typically cost 1% to 4% of the total investment (i.e., at base year; Xu, 1987). These costs mainly comprise the maintenance and replacement of equipment, material purchases and updates, maintenance of the hydropower stations themselves (e.g., line fault and rust prevention), and daily operation. Following previous research (Yang, 2004), combined with the actual state of hydropower station construction in China (e.g., completion quality, acceptance level), the maintenance costs for the 50 hydropower stations were found to be relatively low, so we set the maintenance and operation costs to 1% of the total initial investment. Using the United States in 2002 as a benchmark for the EIO-LCA model (Hendrickson, 2006), we then obtained the flexible price in

Table 1
Carbon emission factors for construction materials (i) and modes of transport (j), used in calculating the carbon footprints of the construction and transportation stages of the hydropower station life cycle.

	Emission factor	Unit	Data source[a]
Type of material (i)			
Concrete	79.0	kg CO_2/t	IPCC[b]
Reinforced steel	2200.0	kg CO_2/t	CIAE[c]
Fuel	142.0	kg CO_2/t	Li et al. (2012b)[d]
Wood	23.9	kg CO_2/t	Garraín et al. (2015)[e]
Explosive substances	543.0	t CO_2/million USD	EIO[f]:Ammunition production
Metal construction	640.0	t CO_2/million USD	EIO[f]:Hardware manufacturing
Electromechanical equipment	644.0	t CO_2/million USD	EIO[f]:Other engine equipment manufacturing
Mode of transport (j)			
Highway	0.184	t/kt·km	NDRC[g]
Railway	0.02215	t/kt·km	NDRC[g]
Waterway	0.024	t/kt·km	NDRC[g]

[a] Data sources:
[b] Intergovernmental Panel on Climate Change (https://www.ipcc.ch/).
[c] China Institute of Atomic Energy (http://www.ciae.ac.cn/index.jsp).
[d] Chinese Life Cycle Database (http://www.ike-global.com/products-2/clcd-intro).
[e] European Life Cycle Database (https://simapro.com/databases/elcd/).
[f] Economic Input-Output (http://www.eiolca.net/).
[g] National Development and Reform Commission (http://www.ndrc.gov.cn).

Table 2
Carbon emission factors for electricity in different provinces, according to Zhixu (2013).

Electrified wire netting	Provinces	Carbon emission factor (kg/kW·h)
North China	Beijing, Tianjin, Hebei, Shanxi, Shandong, Western Inner Mongolia	1.25
Northeastern Region	Liaoning, Jilin, Heilongjiang, Eastern Inner Mongolia	1.10
East China	Shanghai, Jiangsu, Zhejiang, Anhui, Fujian	0.93
Central China	Henan, Hubei, Hunan, Jiangxi, Sichuan, Chongqing	0.80
Northwest Region	Shaanxi, Gansu, Qinghai, Ningxia, Xinjiang	0.98
Southern Region	Guangdong, Guangxi Autonomous Region, Yunnan, Guizhou	0.71
Hainan Province	Hainan	0.92

2002 based on the producer price index (PPI) and the total initial investment (see Table 3 for sources). As a base year, we used the initial year of construction, by using the PPI and purchasing power parity (PPP) from 2002. Combined with additional parameters (see Table 3), we also estimated the GHG emissions in 2002. Finally, with the intensity of GHG emissions as the proportional factor, we calculated China's GHG emissions during the respective hydropower station's base year from the output of the EIO-LCA model. The conversion formula is as follows (see Appendix B for nomenclature):

$$P_{2002} = P_n \times \frac{PPI_{2002}}{PPI_n} \tag{16}$$

$$E_{2002} = \frac{P_{2002}}{PPP} \times F_n \tag{17}$$

$$E_n = E_{2002} \times \frac{I_n}{I_{2002}} \tag{18}$$

To calculate the second portion of the operation stage, CF_{net}, we divided the measure of GHG flux in the reservoir water bodies into two parts: (1) the total flux from the reservoir water bodies (CF_r) and (2) the GHG flux in the basin prior to water storage (CF_i). Adopting the formula from Gagnon and Van (1997), we calculated CF_{net} as:

$$CF_{net} = CF_r - CF_i - CF_p \tag{19}$$

The additional parameter, CF_p, is an estimate of the human CF. Here, since the hydropower stations were generally built in remote areas with little to no human activity (Li et al., 2017a), and economic development was relatively small with low population densities, we assumed that human activities would have very small impacts on hydropower stations in China. We thus assigned a value of 0 to CF_p to exclude it from the calculation.

To calculate CF_r, we used the GHG Risk Assessment Tool (Beta Version; United Nations Educational, Scientific and Cultural Organization International Hydropower Association; Goldenfum). This tool models and estimates the total GHG release of freshwater hydropower stations. The parameters required by the model are the age of the reservoir, mean annual temperature, mean annual runoff depth and mean annual rainfall.

As there were different land cover types in the reservoir areas prior to water storage, we used Landsat TM8 satellite imagery (https://landsat.usgs.gov/landsat-8) to identify them for each area. These land cover types included plowed land, forest, woodland, gardens and water bodies (Lou et al., 2004; Penman, 1948; Zhang et al., 2005; Zhao et al., 2011). The GHG emissions of each land cover type are listed in Table 4, which we obtained by multiplying the carbon emission factor of the respective land cover type by the area it covered in each reservoir (Yang and Zhang, 2016). We then estimated CF_i by taking the sum of the CO_2 and CH_4 fluxes for the different land cover types of each reservoir. Positive sums indicated carbon (CO_2) sources, while negative values indicated carbon sinks. We then used a method adapted from Varis et al. (2012) to convert the CH_4 flux to its CO_2 equivalent, with a global warming potential factor (GWP) of 28 (Lu, 2015). We thus calculated CF_i as follows (see Appendix B for formula nomenclature):

$$CF_i = E_{CO_2} + E_{CH_4(\text{in } CO_2 \text{equivalent})} = E_{CO_2} + E_{CH_4} \times GWP \tag{20}$$

We calculated CF_d as 10% of the total CF from the material production, transportation and construction stages. (Zhang et al., 2007):

$$CF_d = (CF_m + CF_t + CF_c) \times 0.1 \tag{21}$$

2.2.3. Hydropower station classification and analysis of the water and carbon footprints

We calculated the total CF and WF of the 50 hydropower stations by taking the sum of the WF_{total} and CF_{total} across each of them.

To analyze the spatial and environmental characteristics of these hydropower stations, we classified the 50 hydropower stations according to various conditions. We grouped the hydropower stations by the type of climate at each location (*tropical monsoon*, *subtropical monsoon*, *monsoon climate of medium latitudes* and *temperate continental*). We also divided all of the hydropower stations' reservoirs into four storage capacity (reservoir size) classes: *large I* (>1 billion m^3), *large II* (0.1to1 billion m^3), *medium* (0.001 to 0.01 billion m^3) and *small I* (0.01 to 0.1 billion m^3; Sheng and Zhong-You, 2010). All of the hydropower stations' locations were also categorized under five large basins, corresponding to the river in which they are located (Bohai Sea basin, Yangtze River basin, Pearl River basin, Lancang River basin, and Yellow River basin). These characteristics are listed for each hydropower station in Appendix A.

Following previous research that calculates annual average CF of reservoirs (Deshmukh et al., 2013; Zhang and Pang, 2015), we also distributed the total CF value over 50 years for each year of the life cycle. We distributed CF to each year to be consistent with WF and analyze the impact of the reservoir's CF.

We calculated and analyzed the product water footprint (PWF) across these characteristics, which is the WF per unit of hydropower generation (m^3/GJ; Liu et al., 2015). To simultaneously evaluate the WF and CF of each hydropower station, we also calculated the product carbon footprint (PCF) in units of tCO_2e/GJ. We analyzed the correlation between the PWF and PCF of each hydropower station. We assigned each hydropower station's PWF as the independent variable, and used the PCF value of the hydropower station as the dependent variable for input into SPSS (IBM Corp., 2017) for regression analysis.

2.3. Methods for uncertainty analysis and sensitivity analysis

2.3.1. Uncertainty analysis in the different parameters

As an effective tool for decision-making process of energy conservation and emission reduction, LCA is widely used in various industries for environmental quantification. In theory, the results of LCA are reliable and effective for decision makers to make the best decisions. In practice, however, the uncertainty of the underlying data can affect the accuracy of the LCA results. Therefore, in recent years, people have emphasized

Table 3
Parameters used in the Economic Input-Output Life Cycle Assessment (EIO-LCA) (Lave, 2006) to estimate the carbon footprint during the materials and production stage of the hydropower station life cycle.

Parameters	Units	Data sources[a]
Produce Price Index (PPI)	–	NBS[b]
Purchase Power Parity (PPP)	–	WorldBank[c]
Greenhouse gas (GHG) emission	(megaton)	CDIAC[d]
GDP based on PPP	million dollars	IMF[e]

[a] Date sources:
[b] National Bureau of Statistics of the People's Republic of China (http://www.stats.gov.cn/).
[c] http://www.shihang.org/.
[d] Carbon Dioxide Information Analysis Center (http://www.treasurer.ca.gov/cdiac/).
[e] International Monetary Fund (http://www.imf.org/external/index.htm).

Table 4
Carbon footprint flux parameters of each land cover type.

Land cover types	CO_2 flux (mg/(m^2·h))	CH_4 flux (mg/(m^2·h))
Plowed land	41.1	−0.012
Woodland, garden plot	−27.4	−0.012
Meadow	180	−0.24
Water bodies	20.5	0.06
Town	180	−0.24
Hardened land	0	0

Table 5a
Reservoir water footprint data quality indicator matrix.

Water footprint parameter	Data quality indicator matrix	DQI fraction
Average temperature	(5,4,5,5,5)	4.8
Average wind speed	(4,5,5,4,5)	4.6
Relative humidity	(5,5,4,5,4)	4.6
Reservoir age	(5,4,3,3,5)	4

Table 5b
Reservoir carbon footprint data quality indicator matrix.

Carbon footprint parameter	Data quality indicator matrix	DQI fraction
Concrete pouring	(4.5.5.4.4)	4.4
Wood usage	(5,4,4,4,4)	4.2
Reinforced steel	(4,4,4,5,4)	4
Explosive fuel	(3,5,4,3,5)	4
Diesel consumption	(4,4,3,5,5)	4.2
Mechanical and electrical engineering	(4,4,4,5,5)	4.4
Metal structure equipment and installation engineering	(5,4,4,4,5)	4.4
Total construction power consumption	(5,4,5,3,4)	4.2
Hydropower station routine maintenance	(4,4,4,3,5)	4

the importance of uncertainty analysis behind the results of LCA (Ciroth et al., 2002; Geisler et al., 2005).

We adopted the hybrid data quality indicator and statistical method (HDS) to analyze the uncertainty of the WF and CF results for each hydropower station (Wang and Shen, 2013). We first referred to a data quality matrix to classify and score the parameters of each stage in the reservoir evaluation model and perform equal weighting (Tables 5a–5b). Based on the data quality score, the data can was then transformed into various forms of probability distributions, which approximates the true distribution of the simulated data and reduces the uncertainty of the data (Kennedy et al., 1997). This study uses the most widely used beta (β) distribution (Tables 6a–6b).

After converting the data quality score into β distribution, according to the literature data and engineering examples, we determined the range of values of the WF and CF parameters, assuming the maximum, minimum and possible values. We inputted the possible values and probability distribution functions in the Crystal Ball software (Goldman, 2002) for simulation analysis. We performed a total of 50,000 simulations and extracted the Monte Carlo simulation results and the possible values and confidence intervals of WF and CF.

2.3.2. Sensitivity analysis for study

We conducted a sensitivity analysis was carried out to examine the effects of various main parameters (Tables 7a–7b) on the results of water and carbon footprints of hydropower stations. We used a sensitivity index (Liu and Ashton, 1998) to quantify how sensitive the results are to the fluctuations in parameters:

$$Sx = (\Delta X/X)/(\Delta P/P) \tag{22}$$

where X is the evaluation index under original conditions, ΔX is the difference of the evaluation index between original and modified conditions, P is the reference value of the parameter, ΔP is the resulting fluctuation value of the parameter variation and Sx represents the sensitivity of the parameter. We conducted sensitivity analysis on reservoir water footprint and carbon footprint respectively. Firstly, we analyzed the sensitivity of the main parameters of each reservoir in 50 reservoirs, and then took the average value of 50 reservoirs and analyzed the sensitivity of its main parameters.

Table 6a
Water consumption probability distribution.

Water consumption related parameters	Beta(α,β)	Range endpoint
Average temperature	(4.5,4.5)	(±15%) = (140.96, 190.71)
Average wind speed	(4.5,4.5)	(±15%) = (15.80, 21.37)
Average relative humidity	(4.5,4.5)	(±15%) = (64.32, 87.02)
Reservoir water surface area	(4,4)	(±15%) = (8.5×10^7, 1.2×10^8)

Table 6b
Carbon emission probability distribution.

Carbon emissions related activities	Beta (α,β)	Range endpoint
Concrete pouring	(4,4)	(±15%) = (66.73, 90.28)
Wood	(4,4)	(±15%) = (1.49, 2.01)
Reinforced steel	(4,4)	(±15%) = (2.74, 3.71)
Explosive fuel	(4,4)	(±15%) = (45.15, 61.0)
Diesel	(4,4)	(±15%) = (3.48, 4.71)
Mechanical and electrical engineering	(4,4)	(±15%) = (17.77, 24.04)
Metal structure equipment and installation engineering	(4,4)	(±15%) = (3.15, 4.26)
Total construction power consumption	(4,4)	(±15%) = (9957.481, 13,471.89)
Hydropower station routine maintenance	(4,4)	(±15%) = (226.98, 307.09)

The sensitivity results are shown in Fig. 2a–e. By recalculating the reservoir water footprint value by ±10%, we found that the deviation of the results was small (<1.5%).

We found that the average temperature is the most sensitive to the results, followed by the average wind speed and reservoir area, while the relative humidity is relatively less sensitive to the reservoir's water footprint results. When the average temperature increases by 10% and the water footprint will increase by 1.175%; the corresponding average temperature will decrease by 10% and the water footprint will be reduced by 1.400%. When the average wind speed is increased by 10%, the result fluctuates by 0.150% in the positive direction; when decreased by 10%, the corresponding result value decreases by 1.090%. For relative humidity, the result will be the opposite. When the relative humidity is increased by 10%, the water footprint results will be reduced by 0.982%, and when the relative humidity is reduced by 10%, the result will be increased by 0.575%.

3. Results

3.1. The hydropower station water footprint (WF)

Fig. 3 shows the WF of the 50 hydropower stations and their geographic distributions. The combined WF_{total} of these stations was 5.50

Table 7a
Water footprint sensitivity analysis results.

Sensitivity	Low value (10% reduction)	High value (10% increase)
Average temperature	−1.400	1.175
Average wind speed	−1.090	0.150
Relative humidity	0.575	−0.982
Reservoir area	−1.00	1.00

Table 7b
Carbon footprint sensitivity analysis results.

Sensitivity	Low value (10% reduction)	High value (10% increase)
Reservoir age	−1.059	1.059
Average temperature	−1.245	1.241
Average annual rainfall	1.457	−1.521
Annual average runoff	−1.141	1.414
Construction power consumption	−1.149	1.149
Material equipment production	−1.479	1.479
Hydropower station routine maintenance	−0.682	0.707

$\times 10^{11}$ m^3. Among these stations, the WF substantially varied. The WF ranged from 1.25×10^6 (Black Mi Peak Pumped Storage Hydropower Station; no. 48) to 8.50×10^{10} m^3 (Three Gorges Hydroelectric Power Station; no. 1). The mean WF was 1.10×10^{10} m^3. The WF for most hydropower stations ranged from 5.0×10^9 to 5.0×10^{10} m^3 (17 stations) and from 5.0×10^8 to 5.0×10^9 m^3 (22 stations). The WF_{total} of each hydropower station is listed in Appendix A.

The source responsible for the largest proportion of the WF in the hydropower station life cycle was reservoir water surface evaporation (99.30 ± 0.10%). The remaining proportion from material production was 0.70 ± 0.08% (Fig. 4).

The reservoir PWF differed among climate types (Nunes et al., 2017; Table 8). Among hydropower stations, the PWF ranged from 2.13 to 8.89 m3/GJ. Among storage types, the average PWF also varied (Table 8). The average PWF across hydropower station basins ranged from 0.09 to 0.3 m^3/GJ. The relationship among the mean values of the PWF by climate was as follows: *subtropical monsoon climate* > *temperate continental climate* > *tropical monsoon climate* > *monsoon climate of medium latitudes* (Table 8). These lowest hydropower station PWF values found in the temperate monsoon climate zone ranged from 0.013 m^3/GJ to 11.87 m^3/GJ, while the average PWF of the hydropower stations in the other three climate zones was approximately 8 m^3/GJ (Table 8).

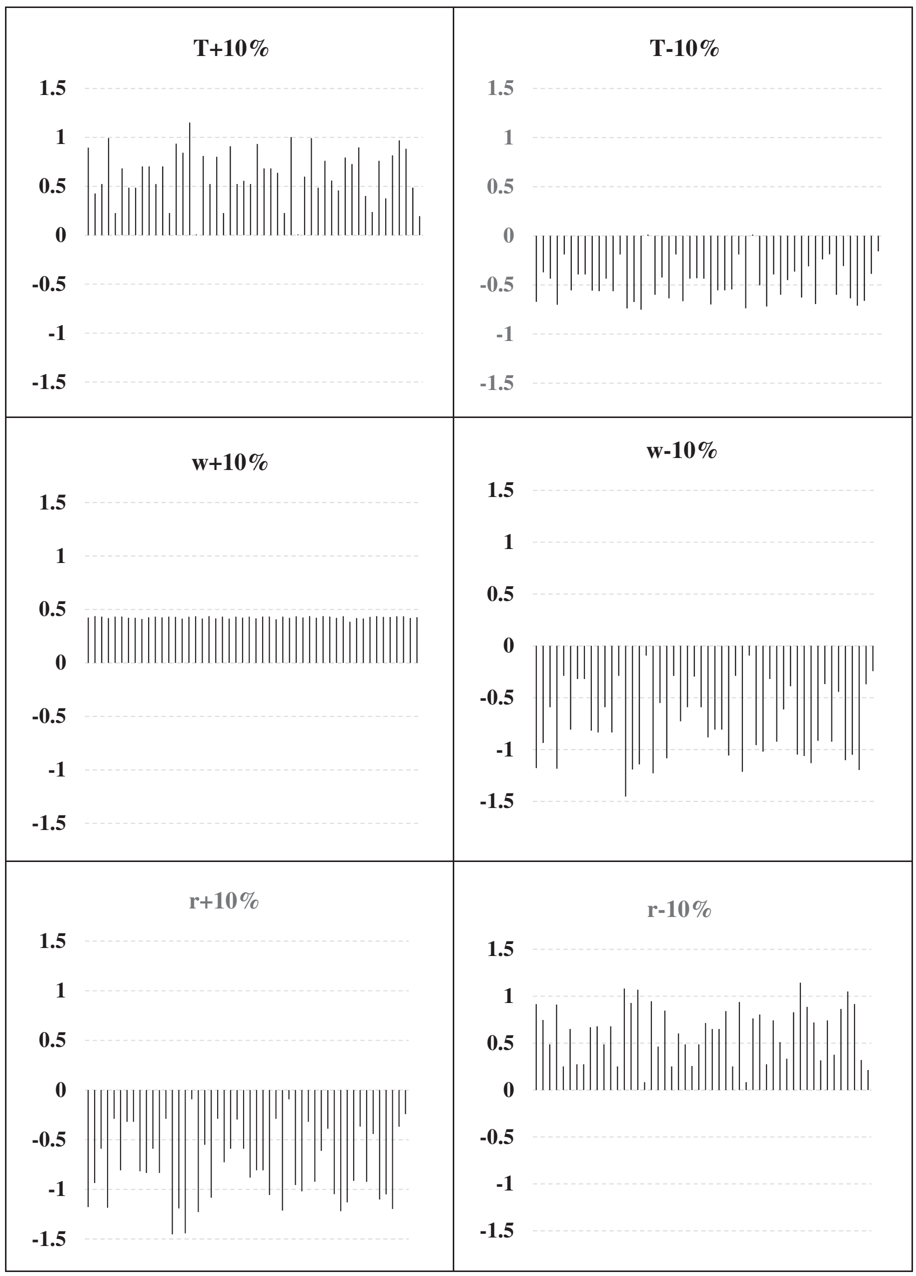

a.

Fig. 2. a. Water footprint sensitivity analysis results (main parameters: average temperature, average wind speed and relative humidity). b. Carbon footprint sensitivity analysis results (Reservoir CH_4 flux: reservoir age, average temperature, average annual rainfall). c. Carbon footprint sensitivity analysis results (Reservoir CO_2 flux: average annual rainfall, reservoir age, annual average runoff). d. Carbon footprint sensitivity analysis results (Secondary parameter: construction, material, routine maintenance). e. Sensitivity analysis of water and carbon footprint results of 50 reservoirs.

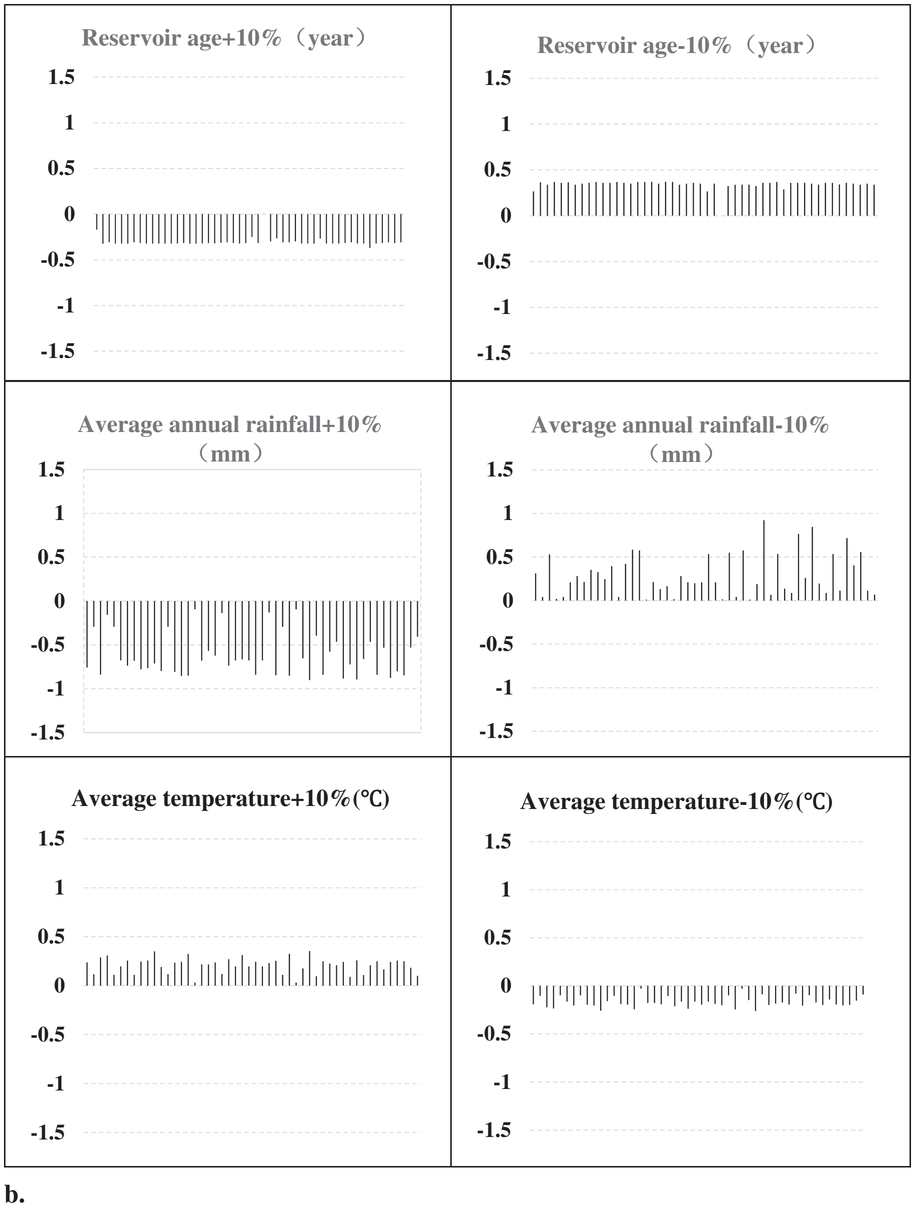

Fig. 2 (*continued*).

3.2. The hydropower station carbon footprint (CF)

The results of the CF analysis of the life cycle of the 50 hydropower stations are shown in Fig. 5. The combined CF_{total}across these stations was $1.06 \times 10^7 tCO_2e$. Among hydropower stations, the CF varied considerably, ranging from 1850 tCO_2e (Panlong Pumped Storage Power Station; no.47) to 89,000 tCO_2e (Three Gorges Hydroelectric Power Station; no.1). The mean CF of these stations was approximately 1.07×10^7 tCO_2e. Most individual CFs ranged from 1850 tCO_2e to 89,000 tCO_2e (26 stations), and from 100,500 tCO_2e to 214,800 tCO_2e (10 stations). The $CF_{total}$of each hydropower station is listed in Appendix A.

Among the life-cycle stages, the operation and maintenance stage had the largest CF, accounting for 87.36% of the CF_{total} across hydropower stations (Fig. 6). The second-largest contribution was from the construction stage, accounting for 8.35% of the combined CF_{total} across hydropower stations. The remaining three stages (raw material and production, material transportation, and dam decommissioning) collectively accounted for <5% of the combined CF_{total} (Fig. 7).

Across the life-cycle stages, storage capacity classes and types of dams, PCF was consistently the largest during the operation and maintenance stage (Figs. 8–9). Across these same categories, we found PCF to be the smallest at the dam decommissioning and transportation stages.

3.3. The relationship between water and carbon footprints

The regression analysis of the PWF and PCF is shown in Fig. 11. The CF was significantly positively correlated with WF in hydropower stations ($p < 0.01$); when the WF of a hydropower station was large, its CF also tended to be large.

3.4. The results of uncertainty analysis and sensitivity analysis

From the distribution map of the uncertainty analysis (Fig. 12), minimum and maximum WF are 2.4×10^7 m^3 and 1.42×10^9 m^3, respectively (95% CI: 2.0×10^8 m^3 to 1.0×10^9 m^3). The minimum and

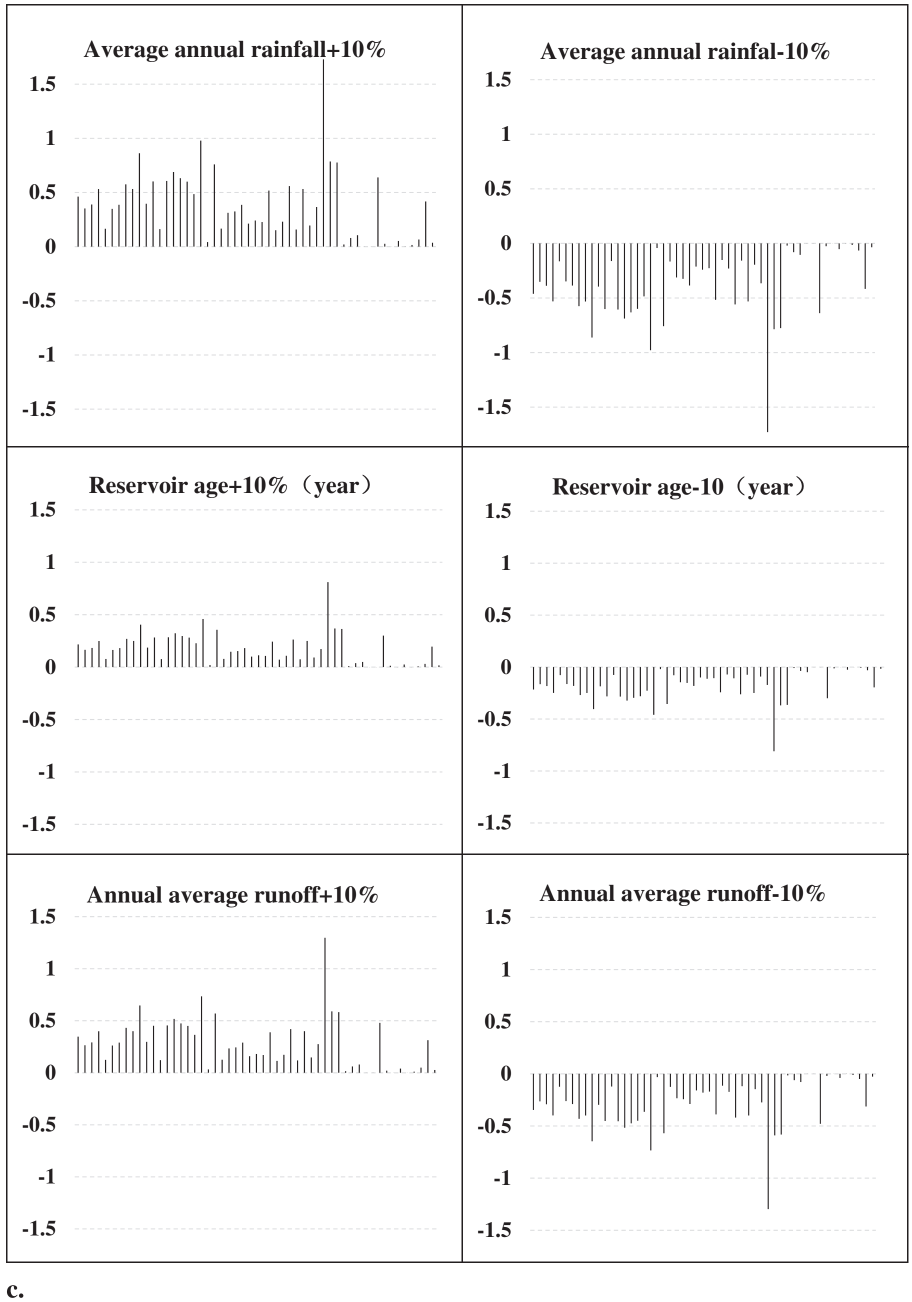

Fig. 2 (*continued*).

maximum CF are 1,295,742 thousand tCO_2e and 1,701,449 thousand tCO_2e, respectively (95% CI: 1.4×10^5 m^3 to 1.6×10^5 m^3). The data results are normally distributed, in line with the actual situation. The CF distribution is small, indicating that the change of parameters has little effect on the results, and the sensitivity of the parameters is small; the distribution of WF is wider, indicating uncertainty of sensitive parameters, having great influence on the simulation results.

The uncertainty of the reservoirs' CF is mainly derived from the GHG emissions of the reservoirs themselves. Since this is a national-scale study, it is difficult to achieve high precision in this part of the data collection. Nevertheless, the emission parameters used in the calculations were from official websites, published books and published papers, giving us confidence in the data quality. The error caused by part of the uncertainty may also be nested in the combination of parameters in the formula calculations of the different stages. However, we collected these parameters from peer-review papers and published books, and we strictly calculated CF based on specifications proposed by the IPCC, making this part of the uncertainty very small.

For the sensitivity analysis of the reservoir CF, we mainly investigated the most important parameters affecting the reservoir carbon emissions. As can be seen from Fig. 2b–c, among these parameters, the GHG emissions of the reservoir itself (mainly related to reservoir age, average temperature, annual average rainfall, annual average runoff depth, etc.) are most sensitive to the results, followed by power consumption during construction and hydropower stations. For daily maintenance, with reservoir age, average temperature and average annual rainfall increase by 10%, respectively; the corresponding carbon emissions will increase by 1.059%, 1.241%, and 1.414% (Table 7b). When

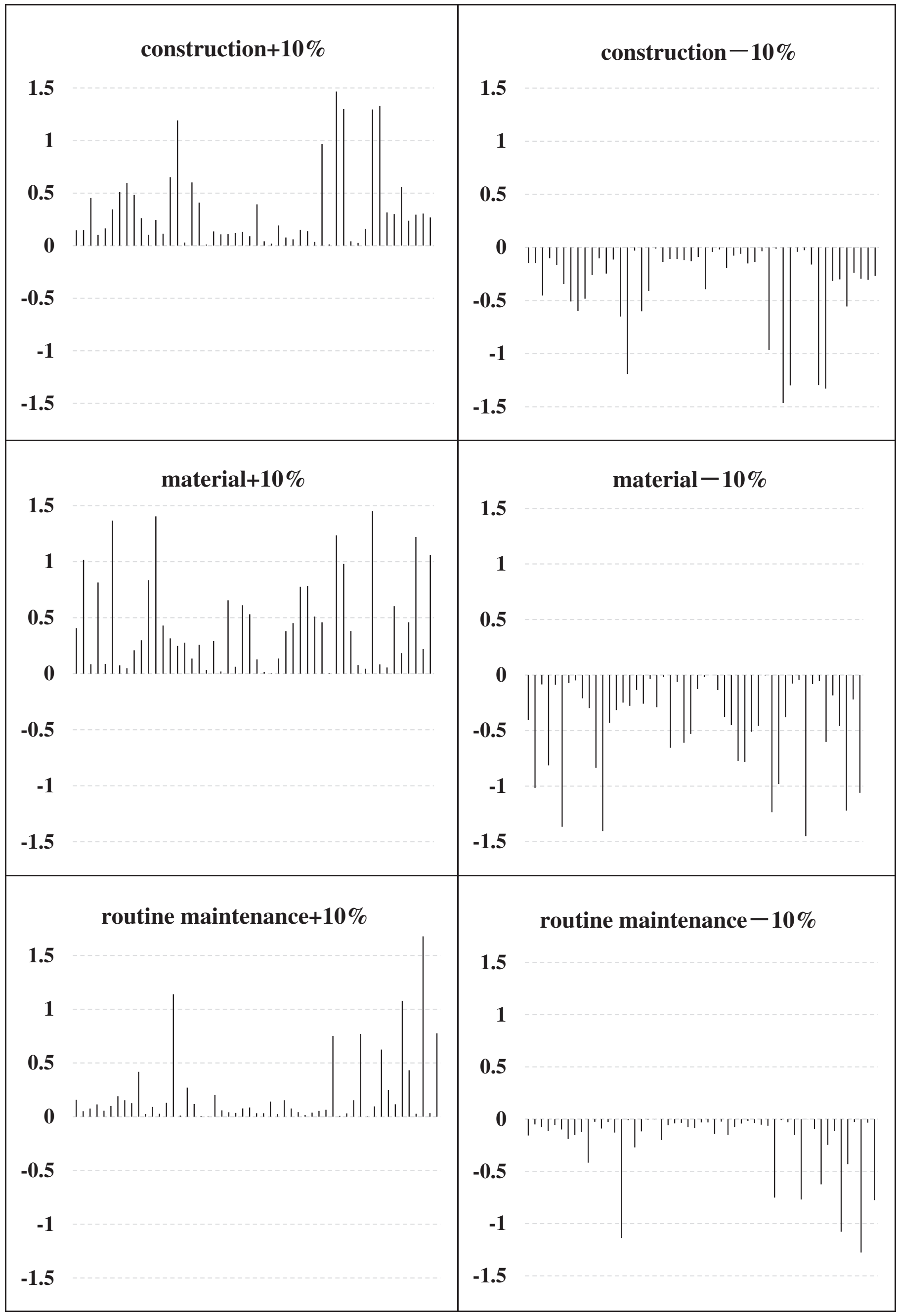

d.

Fig. 2 (*continued*).

these parameters are reduced by 10%, carbon emissions will be reduced by 1.059%, 1.245%, and 1.141%. Fluctuations in annual precipitation are the opposite; increasing precipitation will reduce carbon emissions by 1.0521%, and reducing precipitation will increase carbon emissions by 1.457%. For the power consumption during the construction phase and the parameters of the two parts of materials and equipment production, respectively, increase by 10%, the corresponding carbon emissions will fluctuate by 1.414% and 1.149%, respectively, and the points will be reduced by 10%, respectively, and the corresponding carbon emissions will be negative. The fluctuation was 1.414% and 1.149%. For the parameter change of routine maintenance of hydropower station, when the parameter increases by 10%, the carbon emission result fluctuates by 0.707%. When the parameter decreases by 10%, the carbon emission result fluctuates by 0.682%.

In short, a certain range of parameter changes will have a slight deviation (<1.5%).

4. Discussion

4.1. Hydropower station water and carbon footprint characteristics

This study presents the first environmental impact assessment to simultaneously include both CFs and WFs at a large, national scale with spatially-explicit components (Bonamente et al., 2016). We developed

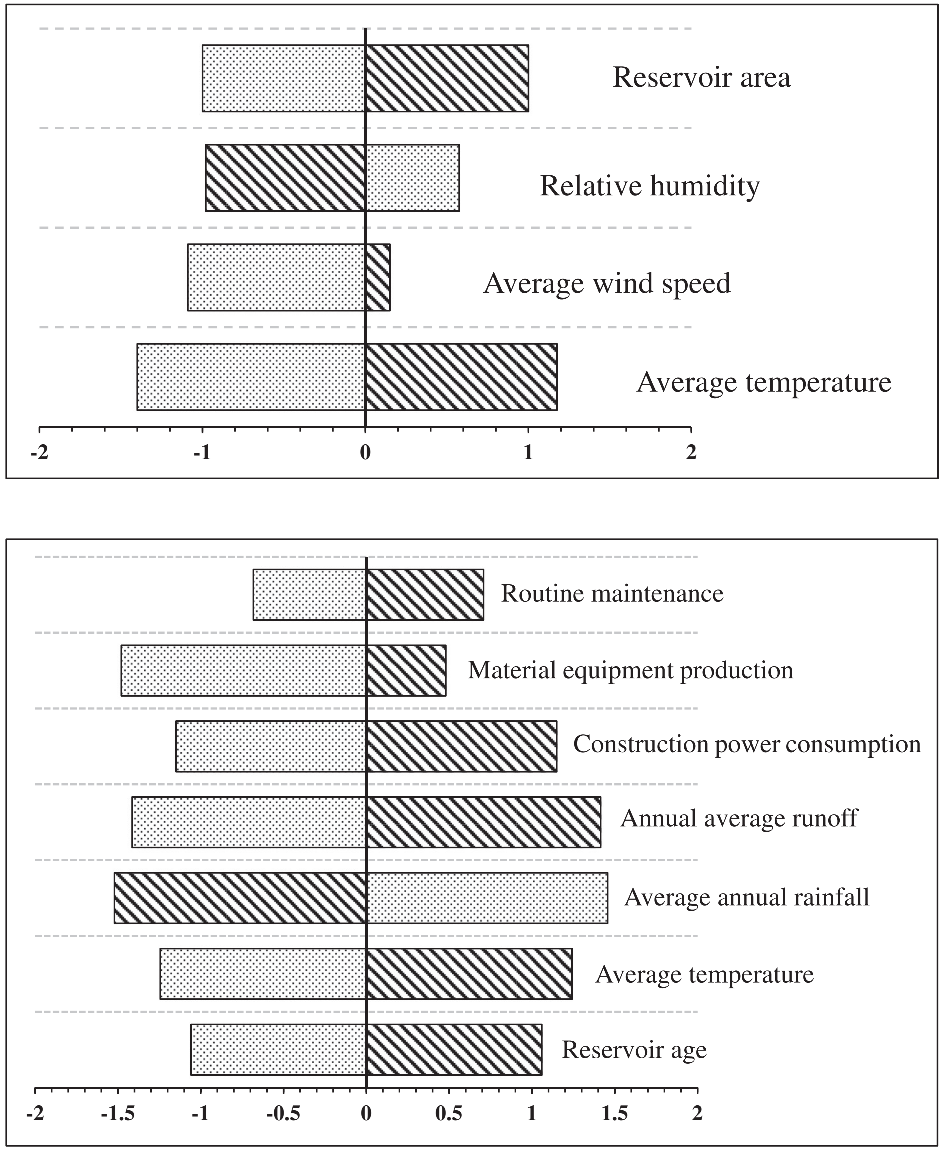

e.

Fig. 2 (*continued*).

a complete environmental impact analysis that included all life-cycle stages of hydropower stations based on LCA theory. The selected 50 hydropower stations together generated over 80% of China's hydropower. From these, we found that the water surface evaporation of hydropower stations accounted for >99% of the WF_{total} across hydropower stations, while material manufacturing accounted for <1%. The CF from the operation and maintenance and construction stages accounted for the largest proportion of the CF_{total}, while <5% of the total CF derived from the raw material and equipment production, transportation, and dam decommissioning stages. These results are similar to Lu (2015), giving us confidence in our findings.

The results of our study indicate that water resource consumption and GHG emissions in the construction and operation of the hydropower stations were still very large. The combined total WF of these hydropower stations was equivalent to 18.9% of Yellow River's annual runoff (Zhang et al., 2009). Considering this, the addition of more hydropower development in the future without regard to its impacts on the environment could aggravate water shortages and climate change. Hydropower as a clean, renewable energy source may therefore have a new challenge to face. In order to reduce its negative impacts on the environment, we must rationally develop and utilize hydropower energy. In the future, assessments about environmental footprints of hydropower stations at a global scale should be conducted to help thoroughly reveal the environmental impacts of hydropower development. Also, future research can set different scenarios to explore the environmental impacts of national hydropower stations under different construction technologies. This would increase the opportunities for policy-makers and managers to decrease the level of negative environmental impacts seen in this study. For example, one possible solution to reduce carbon emissions could be to use low-carbon, environmentally-friendly, water-saving and recyclable materials (Zhuo et al., 2019).

4.2. WF and CF under different classifications

We found that the PWF was largest for subtropical monsoon climates, followed by temperate continental climate, tropical monsoon

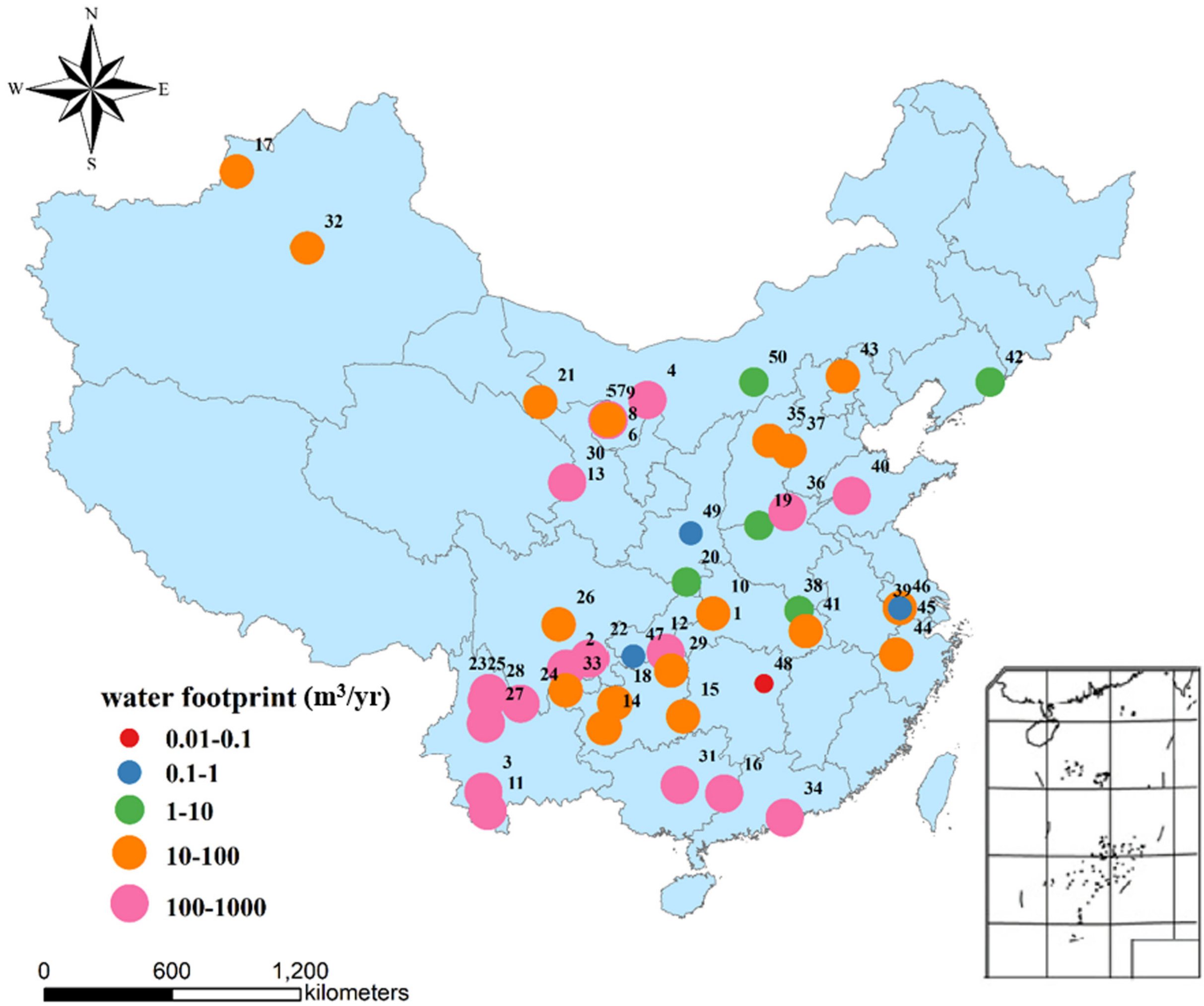

Fig. 3. Water footprint distribution of the 50 hydropower stations. The numbers assigned to each hydropower station correspond to Appendix A, where each hydropower station's water footprint is listed.

climate and monsoon climate of medium latitudes (Table 8). This pattern is possibly because the temperate monsoon climate is in rotating control by winter and summer monsoons. There is a cold and dry climate in the winter, while temperatures in the summer are high, and

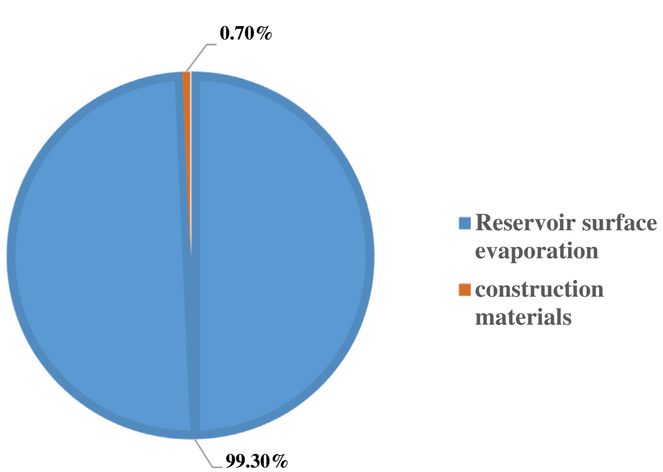

Fig. 4. Water footprint from different parts of the 50 hydropower stations' life cycle.

rainfall is mainly concentrated during the later months. Also, hydropower stations with larger reservoirs always had a larger PWF, as expected for the amount of water being evaporated due to the reservoir's size. This was an advantage to medium-sized hydropower stations; although their reservoirs' storage capacities are relatively small, their installed capacity and annual generated power are large, resulting in a small PWF.

We found that among drainage basins, the PWF of hydropower stations in the Bohai Sea basin were the largest, while the PWF Pearl River basin were the smallest (Table 8). This is possibly because the Bohai Sea basin belongs to the temperate East Asian monsoon climate zone. Spring is affected by the Mongolian continental air mass, resulting in quickly rising temperatures and high wind speeds. Moreover, its climate is dry and often forms arid weather, which results in a large evaporation capacity rate. In summer, it is affected by the neighboring oceanic air mass, with greatly varied rainfall which sometimes results in droughts and flooding. Such climatic characteristics drive the large amount evaporation of hydropower stations in the Bohai Sea basin. The Yangtze River basin features a subtropical monsoon climate, with a hot and rainy summer and cold rain in the winter. Zhuhai basin's temperature does not change intensely, and its rainfall is abundant, which likely drives our finding that the PWF of hydropower stations in this area are smaller. This is consistent with the calculation and analysis of PWFs by Yang et al. (2015).

Table 8
Product water footprints (PWF) under different classifications.

	Climate type	Installed capacity (MV)	No. of stations	Average PWF (m^3/GJ)
Climate	Subtropical monsoon climate	10,030	5	8.89
	Temperate continental climate	2021	4	8.08
	Tropical monsoon climate	93,938	31	7.79
	Monsoon climate of medium latitudes	12,640	10	2.13
	Storage class	**Installed capacity (MV)**	**No. of stations**	**Average PWF (m^3/GJ)**
Reservoir storage capacity	Large I	3787.8	22	11.1
	Large II	1159.7	12	5.70
	Medium	1028.6	7	3.81
	Small I	1575.6	9	2.42
	Drainage basin	**Installed capacity (MV)**	**Generating capacity (billion kW·h)**	**Average PWF (m^3/GJ)**
Drainage basin	Bohai Sea Basin	1100.0	1.74	0.30
	Lancang Basin	3933.3	16.92	0.23
	Yellow River Basin	1898.7	6.94	0.15
	Yangtze River Basin	2748.4	11.12	0.15
	Pearl River Basin	1510.0	3.78	0.09

We found that regardless of classification method, the CF in the operation and maintenance stage was the largest, followed by the construction and material stages (Figs. 7–10); the CF of the transportation and dam decommissioning stages was small enough to be almost negligible. A large CF in the operation and maintenance stage was expected, as it was the most important and the longest part of the hydropower station life cycle, followed by the construction stage, and they both also have many energy and material-intensive requirements. The corresponding CF is therefore large, and the rest of the stages have a short span in the life cycle with a smaller CF.

4.3. The water and carbon footprint relationship

Through a regression analysis of the PWF and PCF, we found a significantly positive relationship between WF and CF (Fig. 10); when the WF of a hydropower station was large, its CF also tended to be large. For

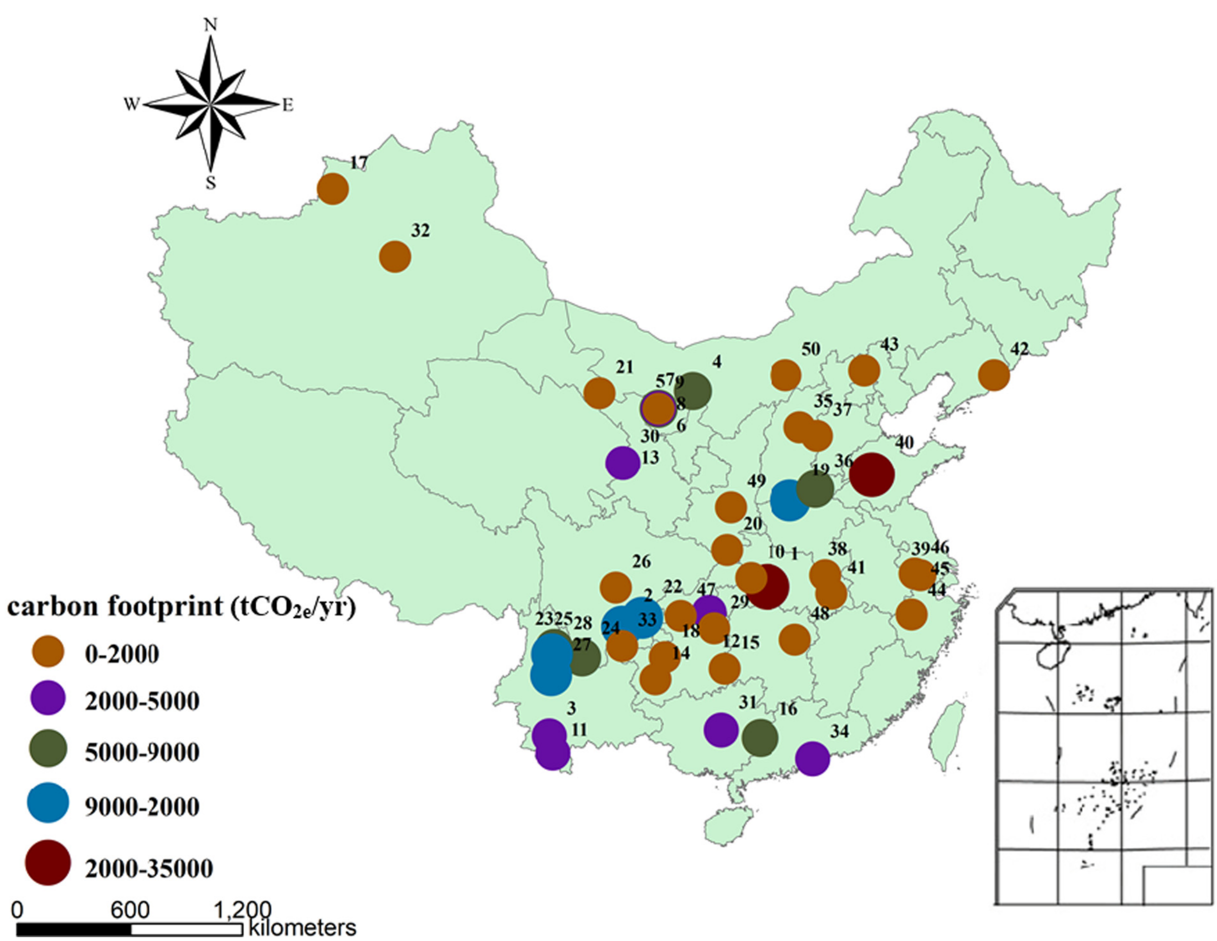

Fig. 5. Carbon footprint of the 50 hydropower stations across their entire life cycle. The numbers assigned to each hydropower station correspond to Appendix A, where each hydropower station's carbon footprint is listed.

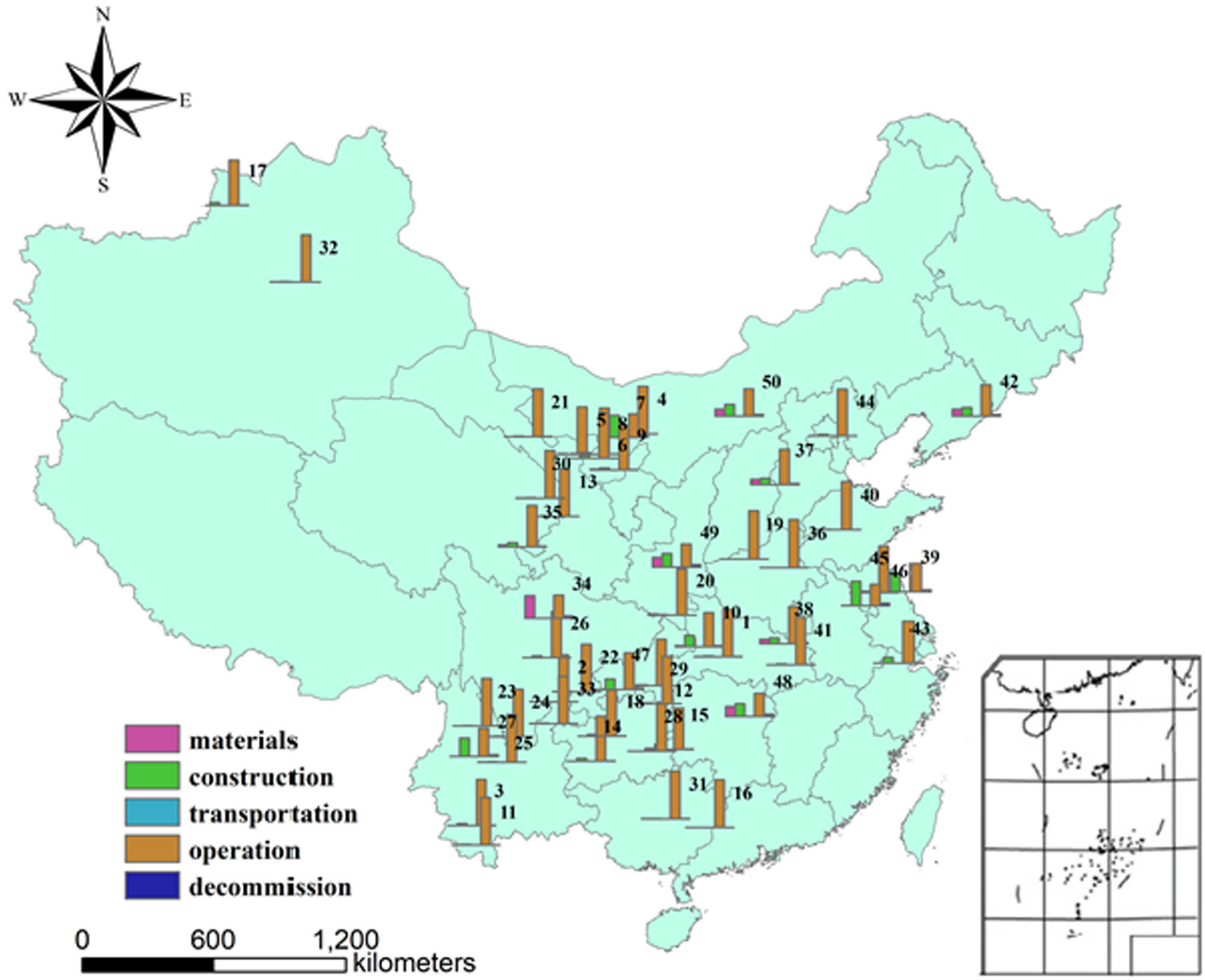

Fig. 6. Proportion of carbon footprint (CF) for each hydropower station's life cycle stage. The height of the bars for each hydropower station represents the ratio between the stages (i.e., a high bar indicates a large CF for that stage, while a low bar indicates a small CF).

example, China's largest power station, Three Gorges Hydroelectric Power Station (no. 1; Appendix A), has both the largest WF and CF among hydropower stations. These results indicate that in order to

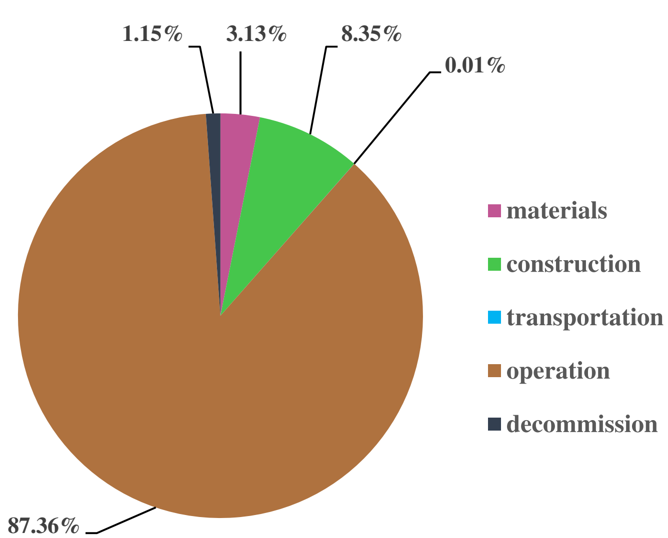

Fig. 7. Proportion of carbon footprint for each life-cycle stage across all 50 hydropower stations.

realize the sustainable development and use of hydropower stations, it is necessary to simultaneously control a hydropower station's carbon emissions (Kumar et al., 2019) and water resource consumption. In this regard, we should focus efforts on reducing both types of environmental impacts together, by reducing the intensity of water consumption and carbon emissions and improving power generation efficiency of hydropower stations.

4.4. Relationship between reservoir construction and water shortage in river basin

The first-level water resources are designated as the nine major rivers, Songliao, Haihe, Yellow, Huaihe, Yangtze, Southeast, Pearl, Southwest and Northwest. The reservoirs in the nine major river basins are unevenly distributed. The number of reservoirs in the Yangtze, Pearl and Yellow Rivers account for >70% of the total, while the reservoirs in the Huaihe, Haihe, and Northwest Rivers are sparsely distributed. The local geographical location, meteorological factors and economic development are closely related. Reservoir construction will have a great impact on local production and living environment and the ecological environment, especially water resources. This study focuses on the impact of reservoir construction on the water shortage in various river basins from the perspective of river basin water resources.

We compared the WF calculation results of 50 representative reservoirs with the effective water consumption of water resources in the

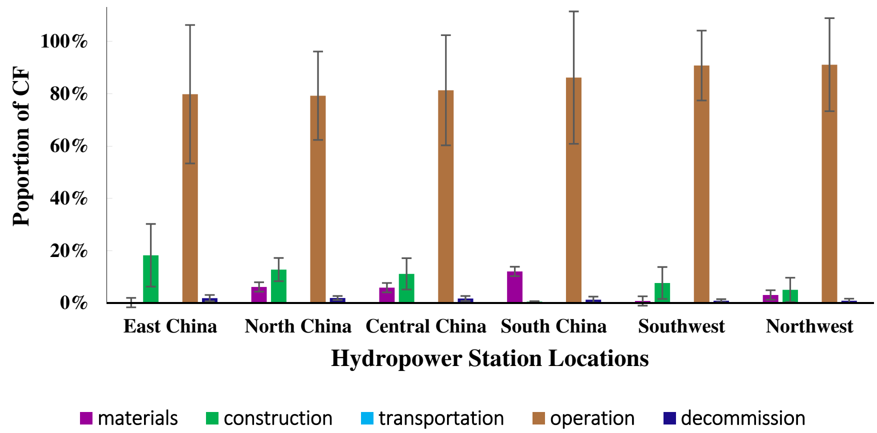

Fig. 8. Proportion of carbon footprint for each hydropower station life-cycle stage in different parts of China.

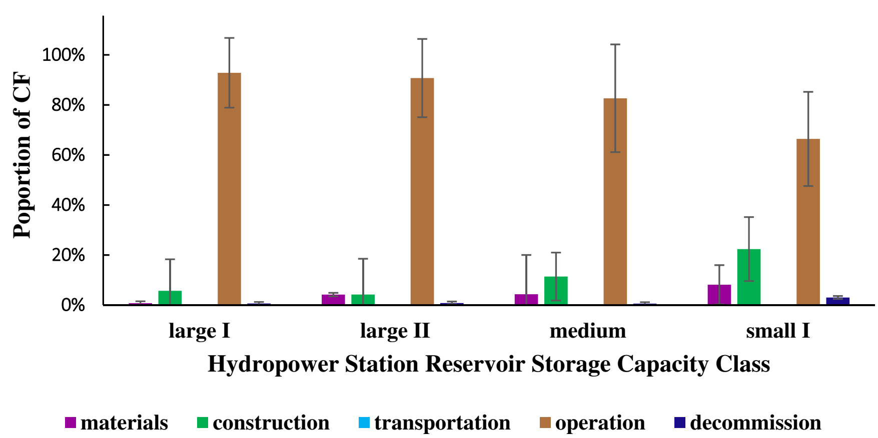

Fig. 9. Proportion of carbon footprint for each hydropower station life-cycle stage according to the reservoirs' storage capacity class.

national basins (Fig. 13). The water resources consumed through nationwide reservoir construction accounted for 0.3103% of the total water resources available, indicating that the construction of these representative reservoirs did not have a serious impact on local water shortage. Therefore, in the future, it is possible to rationally develop and utilize reservoir resources to better solve local practical problems (Table 9).

As the second-largest river, Yellow River runoff is only 65.9 billion m^3, ranking only fourth in the country, and the average annual water resources is only 2% of the country (Liu et al., 2014). In addition, the

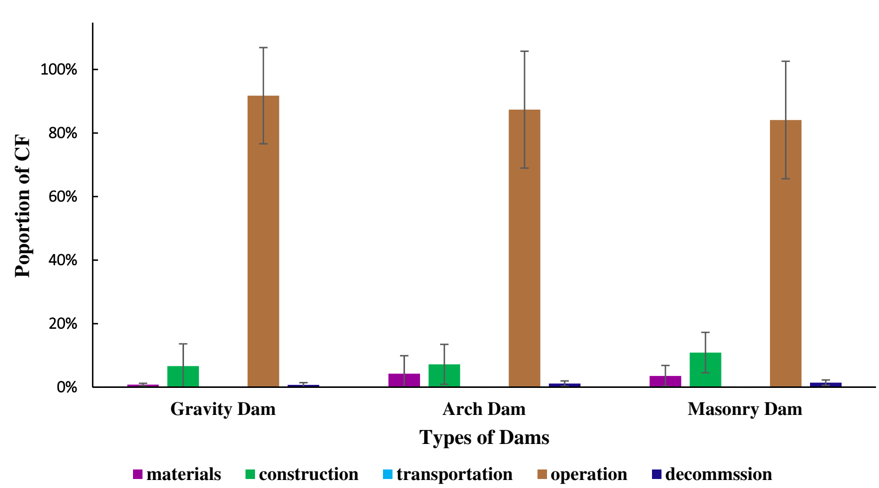

Fig. 10. Proportion of carbon footprint across hydropower stations of different types of dams.

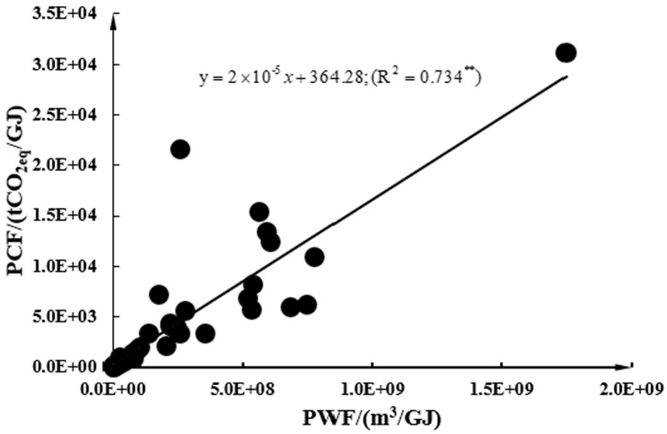

Fig. 11. The regression relationship between the water and carbon footprints of each of the 50 hydropower stations, where the product water footprint (PWF) is the independent variable, and the product carbon footprint (PCF) is the dependent variable. (**: extremely significant; $p < 0.01$).

Yellow River has poor water quality and large sediment concentration, which leads to the small water consumption of the Yellow River, low water shortage and fragile water resources (Jia et al., 2006). The water consumption of reservoirs in the Yellow River basin accounts for 18.98%. When reservoirs are built in the Yellow River in the future, it is important that water consumption is considered. Reservoirs with a smaller WF could instead be selected to alleviate water resources in the Yellow river. For the Southwestern river, due to its complex topography (Zhao, 2011), large area, small population, backward economic and social development, and low level of water resources development and utilization, water consumption from reservoir construction accounted for a higher amount of the water resources. This shows the importance of considering water consumption in the construction stage. In future reservoir development and construction, it is necessary to fully consider reservoir water consumption indicators, rational development and utilization, and also reduce the WF of the reservoir by improving technology.

Due to the limitation of data and methodology, current research doesn't explore the impacts of hydropower development at water quality on a national scale. But water quality has important implications for biodiversity, ecosystem services, and even socioeconomic development. Considering the great significance of this topic, we are eager to fill this knowledge gap in future after we collect enough data.

5. Conclusion

To our knowledge, this study provides the first environmental impact assessment to simultaneously include the WF and CF of multiple influential hydropower stations at a large scale. We were able to show spatial variation in their environmental impacts from different stages of the hydropower station life cycle and potential causes of these variations and impacts.

In this study, we found that the total water loss and carbon emissions from hydropower stations at a national scale are substantial. Central governments should not overlook such a large environmental impact, and should support more scientific research aimed at comprehensively exploring the environmental impacts of hydropower stations at national scales to get a more holistic understanding of hydropower generation. This study can be used as an example for further research on hydropower stations in other nations in the future, as we demonstrate the use of multiple models and tools to calculate water resource consumption and GHG emissions. Our results show that the CF of the operation and maintenance stage accounted for most of the hydropower stations' total carbon emissions, while the WF mainly originated from reservoir water surface evaporation. Based on these findings, we suggest that governments pay special attention to the operation and maintenance stage and water surface evaporation to reduce carbon emissions and water loss, respectively. Furthermore, since water loss and carbon emissions are significantly positively correlated to each other, governments should focus on both impacts simultaneously, as one large footprint likely indicates large environmental impacts from the other footprint. Thus, more cross-sectoral cooperation should be constructed among different departments within governments to address this issue. A more integrated management policy for hydropower that considers multiple kinds of environmental impacts should be developed to maximize the efficiency of hydropower management, further sustainable development and to further its continual, efficient utilization.

Supplementary data to this article can be found online at https://doi.org/10.1016/j.scitotenv.2019.04.148.

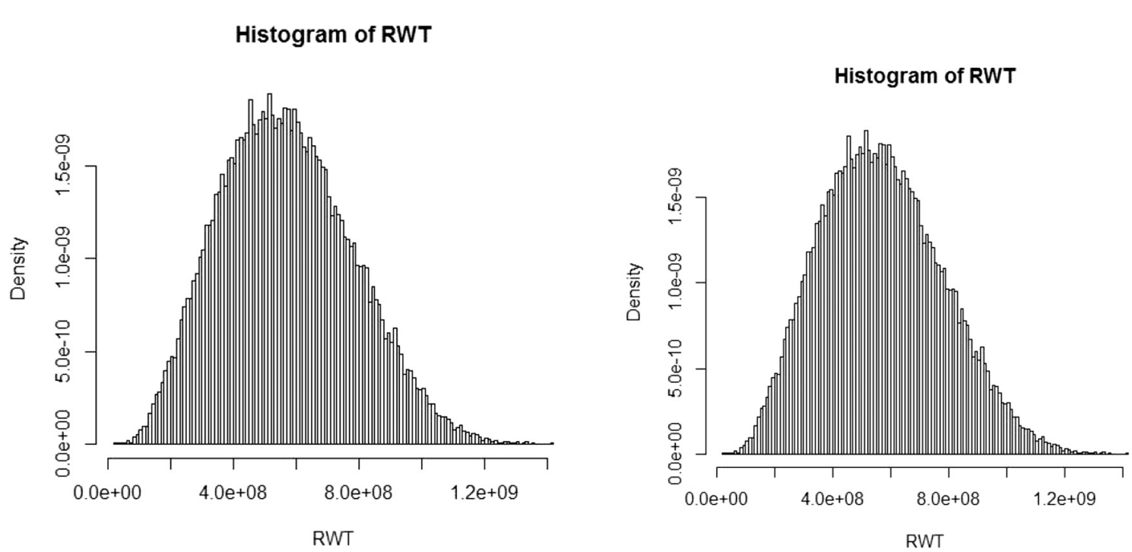

Fig. 12. Monte Carlo simulation results for reservoir water carbon footprint (the horizontal axis represents the simulation results of the reservoir water and carbon footprint, and the vertical axis represents the frequency).

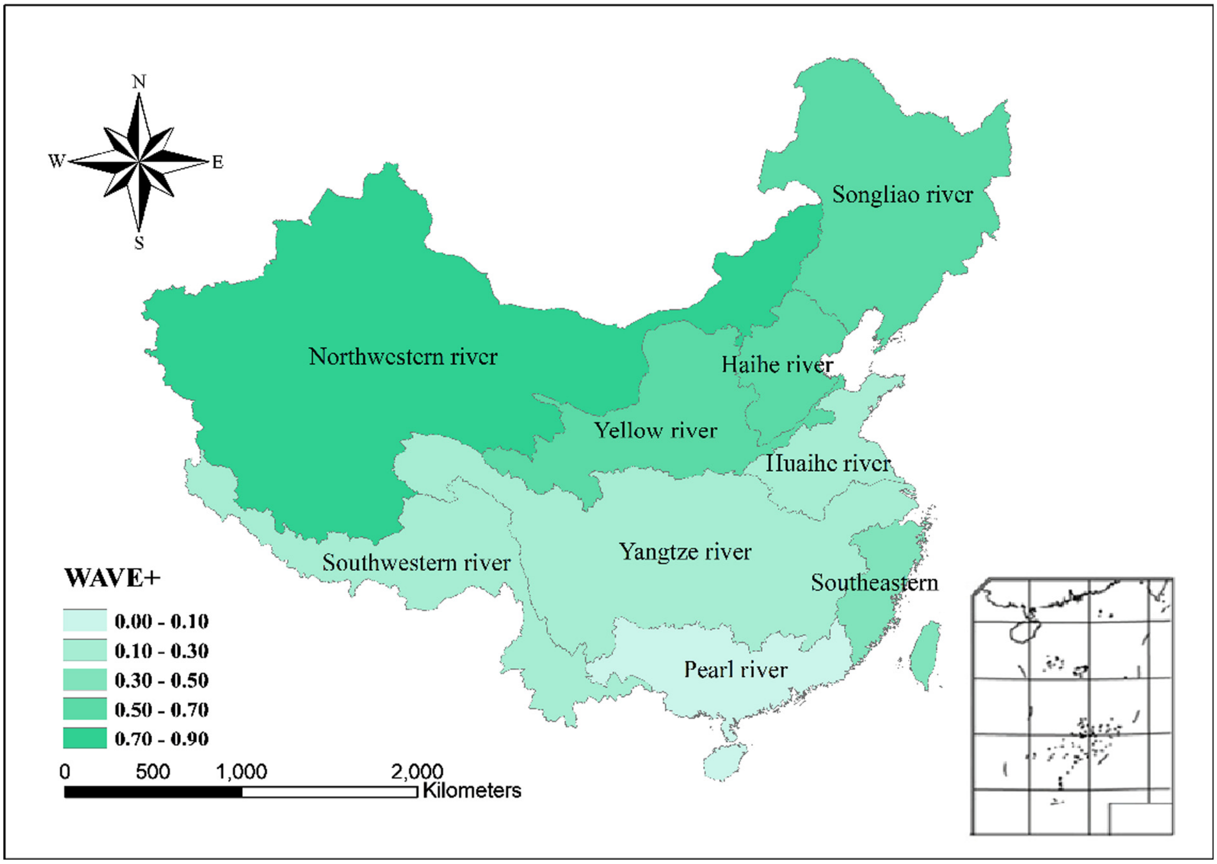

Fig. 13. Nine major rivers distributions and WAVE+ distribution.

Table 9
Water resources and reservoir characteristics in different river.

River	Number	WF (10^7m^3)	WC (10^9m^3)	WC/WF	WAVE+	WDI	BIER$_{\text{-runoff}}$
Songliao river	1	0.01	119.51	0.0001%	0.55	0.56	0.01
Haihe river	4	23.36	155.47	0.1502%	0.67	0.79	0.01
Yellow river	6	103.98	50.92	2.0421%	0.57	0.68	0.04
Huaihe river	1	25.90	342.52	0.0756%	0.28	0.28	0.03
Yangtze river	21	586.32	1676.35	0.3498%	0.27	0.28	0.04
Southeastern	1	5.18	50.92	0.1018%	0.38	0.38	0.02
Pearl river	3	112.99	724.10	0.1560%	0.08	0.08	0.05
Southwestern river	3	174.76	8.16	21.4218%	0.18	0.18	0.06
Northwestern river	10	143.88	663.26	0.2169%	0.79	0.80	0.01
Total	50	1176.39	3791.20	0.3103%	0.40	0.53	0.03

Note: WC: effective water consumption of water resources; WAVE+: vulnerability of watersheds affected by lack of freshwater resources; WDI: water shortage index; BIER-$_{\text{runoff}}$: watershed runoff evaporation rate; WF/WC: reservoir water consumption accounts for effective water consumption of water resources.

Acknowledgements

This work was supported by the National Natural Science Foundation of China (grant number 51621061, 51321001). We thank Thomas Connor for his helpful edits to paper's language.

References

Barnaby, W., 2009. Do nations go to war over water? Nature 458, 282–283.
Bonamente, E., Scrucca, F., Rinaldi, S., Merico, M.C., Asdrubali, F., Lamastra, L., 2016. Environmental impact of an Italian wine bottle: carbon and water footprint assessment. Sci. Total Environ. 560-561, 274–283.
Bribián, I.Z., Capilla, A.V., Usón, A.A., 2011. Life cycle assessment of building materials: comparative analysis of energy and environmental impacts and evaluation of the eco-efficiency improvement potential. Build. Environ. 46 (5), 1133–1140.
Bueno, E.D.O., Mello, C.R.D., Alves, G.J., Bueno, E.D.O., Mello, C.R.D., Alves, G.J., 2016. Evaporation from Camargos hydropower plant reservoir: water footprint characterization. Rbrh 21 (3), 570–575.
Chapagain, A.K., Hoekstra, A.Y., 2002. Virtual water trade: a quantification of virtual water flows between nations in relation to international crop trade. J.org.chem 11 (7), 835–855.
Ciroth, A., Hagelüken, M., Sonnemann, G.W., Castells, F., Fleischer, G., 2002. Geographical and technological differences in Life Cycle Inventories shown by the use of process models for waste incinerators. Int. J. Life Cycle Assess. 7, 363–368.
Delucchi, M.A., Jacobson, M.Z., 2011. Providing all global energy with wind, water, and solar power, part II: reliability, system and transmission costs, and policies. Energy Policy 39 (3), 1170–1190.
Deshmukh, C., Guérin, F., Delon, C., Pighini, S., Vongkhamsao, A., Descloux, S., Chanudet, V., Tardif, R., Godon, A., Guédant, P., 2013. The net GHG (CO2, CH4 and N2O) footprint of a newly impounded subtropical hydroelectric reservoir: Nam Theun 2. EGU General Assembly, p. 10815.

Edenhofer, O., Seyboth, K., Creutzig, F., Schlömer, S., 2013. On the sustainability of renewable energy sources. Annu. Rev. Environ. Resour. 38, 169–200.
Fthenakis, V., Kim, H.C., 2010. Life-cycle uses of water in U.S. electricity generation. Renew. Sustain. Energy Rev. 14 (7), 2039–2048.
Gagnon, L., Van, d.V.J.F., 1997. Greenhouse gas emissions from hydropower. Energy Policy 25 (1), 7–13.
Galli, A., Wiedmann, T., Ercin, E., Knoblauch, D., Ewing, B., Giljum, S., 2012. Integrating ecological, carbon and water footprint into a footprint family of indicators: definition and role in tracking human pressure on the planet. Ecol. Indic. 16 (16), 100–112.
Garraín, D., Fazio, S., Rúa, C.D.L., et al., 2015. Background qualitative analysis of the European reference life cycle database (ELCD) energy datasets – part II: electricity datasets. Springerplus 4 (1), 1–14.
Gerbensleenes, P.W., Hoekstra, A.Y., Meer, T.V.D., 2009. The water footprint of energy from biomass: a quantitative assessment and consequences of an increasing share of bio-energy in energy supply. Ecol. Econ. 68 (4), 1052–1060.
Gleick, P.H., 1992. Environmental consequences of hydroelectric development: the role of facility size and type. Energy 17 (8), 735–747.
Gleick, P.H., 1993. Water in Crisis: A Guide to the World's Fresh Water Resources. New York New York Oxford University Press.
Goldenfum, J.A., GHG Risk Assessment Tool (Beta Version) User Manual.
Goldman, L.I., 2002. Crystal ball software tutorial:crystal ball professional introductory tutorial. Winter Simulation Conference: Exploring New Frontiers.
Herath, I., Deurer, M., Horne, D., Singh, R., Clothier, B., 2011. The water footprint of hydroelectricity: a methodological comparison from a case study in New Zealand. J. Clean. Prod. 19 (14), 1582–1589.
Hendrickson, C.T., Lave, L.B., Matthews, H.S., 2006. Environmental life cycle assessment of goods and services. Nihon Heikatsukin Gakkai Zasshi. 4, pp. 2606–2613.
Hertwich, E.G., Gibon, T., Bouman, E.A., Arvesen, A., Suh, S., Heath, G.A., Bergesen, J.D., Ramirez, A., Vega, M.I., Shi, L., 2015. Integrated life-cycle assessment of electricity-supply scenarios confirms global environmental benefit of low-carbon technologies. Proc. Natl. Acad. Sci. U. S. A. 112 (20), 6277–6282.
Hung, M.L., Ma, H.W., 2009. Quantifying system uncertainty of life cycle assessment based on Monte Carlo simulation. Int. J. Life Cycle Assess. 14, 19–27.
IBM Corp, 2017. . Released. IBM SPSS Statistics for Windows, Version 25.0. IBM Corp, Armonk, NY.
International Energy Agency, 2015. World Energy Outlook 2015. IEA, Vienna.
ISO, 2006. ISO 14064. Greenhouse Gases - Part 1: Specification With Guidance At The Organization Level For Quantification And Reporting Of Greenhouse Gas Emissions And Removals.
Jia, Y., Wang, H., Zhou, Z., Qiu, Y., Luo, X., Wang, J., Yan, D., Qin, D., 2006. Development of the WEP-L distributed hydrological model and dynamic assessment of water resources in the Yellow River basin. J. Hydrol. 331, 606–629.
Kennedy, D.J., Montgomery, D.C., Rollier, D.A., Keats, J.B., 1997. Data Quality. Int. J. Life Cycle Assess. 2, 229–239.
Kumar, A., Yang, T., Sharma, M.P., 2019. Long-term prediction of greenhouse gas risk to the Chinese hydropower reservoirs. Sci. Total Environ. 646, 300–308.
Lave, Lester, B., 2006. Environmental life cycle assessment of goods and services. Resources for the Future.
Li, Hua, Chen, Xiaoyan, Dai, Lingquan, 2009. The Analysis of Fluxes of Greenhouse Gas from the Terrestrial, Aquatorium and Estuary Natural Ecological System. Disaster & Control Engineering.
Li, Z., Du, H., Xiao, Y., Guo, J., 2017a. Carbon footprints of two large hydro-projects in China: life-cycle assessment according to ISO/TS 14067. Renew. Energy 114.
Li, X., Gong, X., Liu, Y., 2017b. Development and application of basis database for materials life cycle assessment in china. IOP Conference Series Materials Science and Engineering, p. 182.
Liu, J., Ashton, P.S., 1998. FORMOSAIC: an individual-based spatially explicit model for simulating forest dynamics in landscape mosaics. Ecol. Model. 106, 177–200.
Liu, K.K., Li, C.H., Cai, Y.P., Xu, M., Xia, X.H., 2014. Comprehensive evaluation of water resources security in the Yellow River basin based on a fuzzy multi-attribute decision analysis approach. Hydrol. Earth Syst. Sci. 18 (5(2014-05-07) 11), 1605–1623.
Liu, J., Zhao, D., Gerbens-Leenes, P.W., Guan, D., 2015. China rising hydropower demand challenges water sector. Sci. Rep. 5, 11446.
Lou, Y., Li, Z., Zhang, T., 2004. CO2 emissions from upland and paddy red soils in mid-subtropical China. Acta Ecol. Sin. 24 (5), 978–983.
Lu, Y., 2015. Greenhouse Gas Emissions From Different Sources of Electricity in China.
Ma, X., Yang, D., Shen, X., Zhai, Y., Zhang, R., Hong, J., 2018. How much water is required for coal power generation: an analysis of gray and blue water footprints. Sci. Total Environ. 636, 547–557.
Mekonnen, M.M., Hoekstra, A.Y., 2011. The water footprint of electricity from hydropower. Hydrol. Earth Syst. Sci. 8 (5), 179–187.
Mekonnen, M.M., Hoekstra, A.Y., 2016. Four billion people facing severe water scarcity. Sci. Adv. 2 (2), e1500323.
Mekonnen, M.M., Gerbens-Leenes, P.W., Hoekstra, A.Y., 2016. Future electricity: the challenge of reducing both carbon and water footprint. Sci. Total Environ. 569–570, 1282–1288.
Min, Q., Zhang, W.K., 2003. Study on the Calculation Method of Reservoir Surface Evaporation. Water Power.
Moomaw, W., Burgherr, P., Heath, G., Lenzen, M., Nyboer, J., Verbrugge, A., 2011a. IPCC special report on renewable energy sources and climate change mitigation. Minerva Cardioangiol. 9 (4), 758–761.
Moomaw, W., Burgherr, P., Heath, G., Lenzen, M., Nyboer, J., Verbruggen, A., 2011b. Annex II: methodology. In IPCC special report on renewable energy sources and climate change mitigation. Minerva Cardioangiol. 9 (4), 758–761.
Nunes, J.P., Jacinto, R., Keizer, J.J., 2017. Combined impacts of climate and socio-economic scenarios on irrigation water availability for a dry Mediterranean reservoir. Sci. Total Environ. 584–585, 219.
Pellicer-Martínez, F., Martínez-Paz, J.M., 2016. The water footprint as an indicator of environmental sustainability in water use at the river basin level. Sci. Total Environ. 571, 561–574.
Peng, C., 2006. China Hydropower Project in the 21st Century.
Penman, H.L., 1948. Natural evaporation from open water, hare soil and grass. Proc. R. Soc. Lond. 193 (1032), 120.
Prairie, Y.T., Alm, J., Beaulieu, J., Barros, N., Battin, T., Cole, J., Giorgio, P.D., Delsontro, T., Guérin, F., Harby, A., 2017. Greenhouse gas emissions from freshwater reservoirs: what does the atmosphere see? Ecosystems 1–14.
Ribeiro, F.D.M., Silva, G.A.D., 2010. Life-cycle inventory for hydroelectric generation: a Brazilian case study. J. Clean. Prod. 18 (1), 44–54.
Rothausen, S., Conway, D., 2011. Greenhouse-gas emissions from energy use in the water sector. Nat. Clim. Chang. 1 (4), 210–219.
Shakya, S.R., Shrestha, R.M., 2011. Transport sector electrification in a hydropower resource rich developing country: energy security, environmental and climate change co-benefits. Energy Sustain. Dev. 15 (2), 147–159.
Sheng, J.B., Zhong-You, F.U., 2010. A comparative study of dam classification between the Chinese method and the international practices. Hydro-Science and Engineering 2 (2), 8–13.
Soito, J.L.D.S., 2011. Amazon and the expansion of hydropower in Brazil: vulnerability, impacts and possibilities for adaptation to global climate change. Renew. Sustain. Energy Rev. 15 (6), 3165–3177.
Varis, O., Kummu, M., Härkönen, S., Huttunen, J.T., 2012. Greenhouse Gas Emissions from Reservoirs.
Wackernagel, M., 1999. Evaluating the use of natural capital with the ecological footprint: applications in Sweden and subregions. Ambio 28 (7), 604–612.
Wang, E., Shen, Z., 2013. A hybrid Data Quality Indicator and statistical method for improving uncertainty analysis in LCA of complex system: application to the whole-building embodied energy analysis. J. Clean. Prod. 43, 166–173.
Wiedmann, T., Minx, J., 2009. A definition of 'carbon footprint'. J. R. Soc. Med. 92 (4), 193–195.
Wüstenhagen, R., Wolsink, M., Bürer, M.J., 2007. Social acceptance of renewable energy innovation: an introduction to the concept. Energy Policy 35 (5), 2683–2691.
Xiaoyong Huang, S.S., Guangcheng, X., 2014. World Energy Development Report (2013).
Xu, Zhifang, S.P., 1987. Water Conservancy Engineering Economics Water Conservancy and Electric Power Press.
Xue, Z., Jiang, Y., 2004. Energy Consumption and Energy Saving Potential Analysis for Large-scale Public Buildings in Beijing. Hv & Ac.
Yang, X., 2004. A brief analysis of the dike in the United States. China Water Resources (13), 15–20.
Yang, Q., Zhang, X., 2016. Improving SWAT for simulating water and carbon fluxes of forest ecosystems. Sci. Total Environ. 569-570, 1478–1488.
Yang, H.E., Chang-Ming, J.I., Shi, P., 2015. Calculation analysis and discussion of blue water footprint for hydropower station. Water Resources & Power.
Yüksel, I., 2009. Hydropower for sustainable water and energy development. Renew. Sustain. Energy Rev. 14 (1), 462–469.
Zhang, S., Pang, B., 2015. Analysis on environmental discharge of large-scale hydropower project using carbon footprint theory. Journal of Hydroelectric Engineering 34, 170–176.
Zhang, Z., Zhu, B., Jiang, C., Han, G., Gao, M., 2005. CO2, N2O and CH4 emission from dryland wheat ecosystem in hilly area of central Sichuan Basin. Chinese Journal of Ecology 24 (2), 131–135.
Zhang, Q., Karney, B., Maclean, H.L., Feng, J., 2007. Life-cycle inventory of energy use and greenhouse gas emissions for two hydropower projects in China. J. Infrastruct. Syst. 13 (4), 271–279.
Zhang, X., Zhang, L., Wang, Y., Mu, X., 2009. Tempo-spatially responses of the annual streamflow to LUCC in the middle reaches of Yellow River, China. Science of Soil & Water Conservation.
Zhang, S., Pang, B., Zhang, Z., 2015. Carbon footprint analysis of two different types of hydropower schemes: comparing earth-rockfill dams and concrete gravity dams using hybrid life cycle assessment. J. Clean. Prod. 103, 854–862.
Zhao, W., 2011. Study on River Basin Development and Human Settlement Environment Construction in Southwest China—A Study on Water Resources and Environmental Assessment and Carrying Capacity. Southeast University Press.
Zhao, D., Liu, J., 2015. A new approach to assessing the water footprint of hydroelectric power based on allocation of water footprints among reservoir ecosystem services. Phys. Chem. Earth 79–82 (3), 40–46.
Zhao, Z., Zhang, Tian, D., Xiang, W., Yan, W., Peng, C., 2011. Characteristics of CO2 flux in a Chinese fir plantation ecosystem in Huitong County, Hunan Province. Sci. Silvae Sin. 47 (11), 6–12.
Zheng, S., 2006. Discussion on hydropower resources development and environmental & ecological protection in China. Eng. Sci. 8 (6), 1–6.
Zhixu, Y.I., 2013. National Greenhouse Gas Emissions Inventory of Agriculture Department in Sichuan Province. Science & Technology Information.
Zhuo, L., Hoekstra, A.Y., Wu, P., Zhao, X., 2019. Monthly blue water footprint caps in a river basin to achieve sustainable water consumption: the role of reservoirs. Sci. Total Environ. 650, 891–899.